Leading Edge
Review

Cell

Evolution of Transcriptional Regulatory Circuits in Bacteria

J. Christian Perez[1,2] and Eduardo A. Groisman[1,*]
[1]Department of Molecular Microbiology, Howard Hughes Medical Institute, Washington University School of Medicine, Campus Box 8230, 660 S. Euclid Avenue, St. Louis, MO 63110, USA
[2]Present address: Department of Microbiology and Immunology, University of California, San Francisco, 600 16th Street, Genentech Hall, Room N374, San Francisco, CA 94143-2200, USA
*Correspondence:groisman@borcim.wustl.edu
DOI 10.1016/j.cell.2009.07.002

Related organisms typically respond to a given cue by altering the level or activity of orthologous transcription factors, which, paradoxically, often regulate expression of distinct gene sets. Although promoter rewiring of shared genes is primarily responsible for regulatory differences among related eukaryotic species, in bacteria, species-specific genes are often controlled by ancestral transcription factors, and regulatory circuit evolution has been further shaped by horizontal gene transfer. Modifications in transcription factors and in promoter structure also contribute to divergence in bacterial regulatory circuits.

Introduction

Free-living organisms typically respond to a change in their surroundings or in cellular components by modifying the expression of multiple genes. In addition to sensors that detect chemical or physical cues and signaling molecules that transduce these stimuli within a cell, the responses to such changes often rely on DNA-binding proteins that interact with specific DNA sequences in promoters to activate or repress gene transcription. Thus, the regulatory circuit defined by the "wiring" between regulatory proteins and target genes determines the repertoire of gene products that an organism synthesizes upon encountering a particular signal or experiencing a developmental cue.

Related species usually rely upon orthologous regulatory systems to orchestrate responses to a given signal. In certain circumstances, the elicited responses are largely similar across species, indicative that orthologous regulatory systems control common cellular functions across species even if the species occupy different niches. In other circumstances, the responses are distinct, either in qualitative or quantitative terms, suggesting that the regulatory systems adopted by individual species are suited to particular habitats and lifestyles.

The different responses that orthologous regulatory systems can elicit when experiencing a given signal indicate that transcription circuits experience modifications in the interactions between regulators and their targets. These modifications may result in abilities that enable organisms to occupy new niches, thus contributing to the phenotypic diversity that exists among related species (McAdams et al., 2004). Yet, the observed rewiring of regulatory circuits does not necessarily result from adaptive processes, even when it causes significant changes in gene expression outputs (Lynch, 2007).

Until very recently, the knowledge of transcription regulatory circuits was limited to a few model organisms belonging to phylogenetically distant groups and sharing relatively few genes. This prevented the comparative analyses of orthologous regulatory circuitries across closely related organisms. Thus, the extent of modifications undergone by regulatory circuitries remained largely unknown. However, the availability of an increasing number of genome sequences, the use of genome-wide computational and experimental approaches to uncover entire sets of regulatory interactions in multiple species, and the engineering of organisms harboring the regulatory architecture from a related species have made it possible to study empirically the patterns of evolution of regulatory circuits. These studies have revealed that differences in regulatory circuitry can play a significant role in the morphological and developmental evolution in animals (Carroll, 2005, 2008; Davidson, 2006), are responsible for the distinct expression of antibiotic resistance determinants in bacteria (Kato et al., 2007; Winfield and Groisman, 2004; Winfield et al., 2005), and may direct the colonization of new niches in unicellular eukaryotic organisms (Borneman et al., 2007; Tuch et al., 2008a). Therefore, tinkering with transcription factors, promoter sequences, and circuit architecture, which are often referred to as "the regulatory genome" (Carroll, 2005, 2008; Davidson, 2006), has given rise to a variety of traits both in bacteria and eukaryotes.

The investigation of bacterial regulatory circuits has focused on a relative small number of extant species (consider that most bacterial species cannot be cultured in the laboratory). Yet, these investigations suggest that the evolution of regulatory circuits in bacteria proceeds in a different manner from what has been described thus far in eukaryotes (Carroll, 2005, 2008; Davidson, 2006; Tuch et al., 2008b). The reasons for the differences are the following: First, unlike closely related eukaryotic organisms, closely related bacterial species exhibit significant differences in gene content due to the pervasiveness of horizontal gene transfer. This means that the spectrum of targets controlled by orthologous transcription factors can be quite different among related bacteria. Moreover, it can cre-

Cell

Theory

Protein Sectors: Evolutionary Units of Three-Dimensional Structure

Najeeb Halabi,[1,4] Olivier Rivoire,[2,4] Stanislas Leibler,[2,3] and Rama Ranganathan[1,*]
[1]The Green Center for Systems Biology, and Department of Pharmacology, University of Texas Southwestern Medical Center, Dallas, TX 75390-9050, USA
[2]The Center for Studies in Physics and Biology and Laboratory of Living Matter, Rockefeller University, New York, NY 10065, USA
[3]The Simons Center for Systems Biology and the School of Natural Sciences, The Institute for Advanced Study, Princeton, NJ 08540, USA
[4]These authors contributed equally to this work
*Correspondence: rama.ranganathan@utsouthwestern.edu
DOI 10.1016/j.cell.2009.07.038

SUMMARY

Proteins display a hierarchy of structural features at primary, secondary, tertiary, and higher-order levels, an organization that guides our current understanding of their biological properties and evolutionary origins. Here, we reveal a structural organization distinct from this traditional hierarchy by statistical analysis of correlated evolution between amino acids. Applied to the S1A serine proteases, the analysis indicates a decomposition of the protein into three quasi-independent groups of correlated amino acids that we term "protein sectors." Each sector is physically connected in the tertiary structure, has a distinct functional role, and constitutes an independent mode of sequence divergence in the protein family. Functionally relevant sectors are evident in other protein families as well, suggesting that they may be general features of proteins. We propose that sectors represent a structural organization of proteins that reflects their evolutionary histories.

INTRODUCTION

How does the amino acid sequence of a protein specify its biological properties? Here, we intend the term "biological properties" to broadly encompass chemical activity, structural stability, and other features that may be under selective pressure. A standard measure of the importance of protein residues is sequence conservation—the degree to which the frequency of amino acids at a given position deviates from random expectation in a well-sampled multiple sequence alignment of the protein family (Capra and Singh, 2007; Ng and Henikoff, 2006; Zvelebil et al., 1987). The more unexpected the amino acid distribution at a position, the stronger the inference of evolutionary constraint and therefore of biological importance. However, protein structure and function also depend on the cooperative action of amino acids, indicating that amino acid distributions at positions cannot be taken as independent of one another (Gobel et al., 1994; Lichtarge et al., 1996; Lockless and Ranganathan, 1999; Neher, 1994). A more informative formulation of sequence conservation should be to include pairwise or even higher-order correlations between sequence positions—the statistical signature of conserved interactions between residues. Indeed, analyses of correlations have contributed to the identification of allosteric mechanisms in proteins (Ferguson et al., 2007; Hatley et al., 2003; Kass and Horovitz, 2002; Lee et al., 2008, 2009; Peterson et al., 2004; Shulman et al., 2004; Skerker et al., 2008) and were found to be sufficient for recapitulating native folding and function in a small protein interaction module (Russ et al., 2005; Socolich et al., 2005).

These findings motivate a deeper theoretical and experimental analysis of correlations of sequence positions with the goal of understanding how protein sequences encode the basic conserved biological properties of a protein family. Here, we carry out this analysis using a classic model system for enzyme catalysis, the S1A family of serine proteases (Hedstrom, 2002; Rawlings and Barrett, 1994; Rawlings et al., 2008). We find that the nonrandom correlations between sequence positions indicate a decomposition of the protein into groups of coevolving amino acids that we term "sectors." In the S1A proteases, the sectors are nearly statistically independent, are physically connected in the tertiary structure, are associated with different biochemical properties, and have diverged independently in the evolution of the protein family. Functionally relevant and physically contiguous sectors are evident in other protein domains as well, providing a basis for directing further experimentation using the principles outlined in the serine protease family. Overall, our data support two main findings: (1) protein domains have a heterogeneous internal organization of amino acid interactions that can comprise multiple functionally distinct subdivisions (the sectors), and (2) these sectors define a decomposition of proteins that is distinct from the hierarchy of primary, secondary, tertiary, and quaternary structure. We propose that the sectors are features of protein structures than reflect the evolutionary histories of their conserved biological properties.

RESULTS

From Amino Acid Sequence to Sectors

The S1A family consists primarily of enzymes catalyzing peptide bond hydrolysis through a conserved chemical mechanism, but

Cell

Transposition into Replicating DNA Occurs through Interaction with the Processivity Factor

Adam R. Parks,[1,3] Zaoping Li,[1] Qiaojuan Shi,[1] Roisin M. Owens,[2] Moonsoo M. Jin,[2] and Joseph E. Peters[1,*]
[1]Department of Microbiology
[2]Department of Biomedical Engineering
Cornell University, Ithaca, NY 14853, USA
[3]Present address: National Cancer Institute Center for Cancer Research, Frederick, MD 21702, USA
*Correspondence: jep48@cornell.edu
DOI 10.1016/j.cell.2009.06.011

SUMMARY

The bacterial transposon Tn7 directs transposition into actively replicating DNA by a mechanism involving the transposon-encoded protein TnsE. Here we show that TnsE physically and functionally interacts with the processivity factor of the DNA replication machinery in vivo and in vitro. Our work establishes an in vitro TnsABC+E transposition reaction reconstituted from purified proteins and target DNA structures. Using the in vitro reaction we confirm that the processivity factor specifically reorders TnsE-mediated transposition events on target DNAs in a way that matches the bias with active DNA replication in vivo. The TnsE interaction with an essential and conserved component of the replication machinery, and a DNA structure reveals a mechanism by which Tn7, and probably other elements, selects target sites associated with DNA replication.

INTRODUCTION

Transposons are genetic elements that are capable of moving from one location to another within a cell. The bacterial transposon Tn7 and its relatives are abundantly distributed among bacteria in a wide variety of medical and environmental settings (Parks and Peters, 2007, 2009). Tn7 has served as a model system for transposition, especially for the understanding of transposon target-site selection (reviewed in Peters and Craig, 2001b; Craig et al., 2002). Target site selection is the process by which transposons assess new DNA molecules for potential insertion. While most transposable elements possess a weak target DNA sequence preference that guides target site selection, Tn7 uses two distinct target site selection pathways. In one pathway a sequence-specific DNA binding protein directs transposition into a single site within the bacterial chromosome and in the other a separate protein recognizes a process associated with DNA replication. These two target selection pathways optimize vertical and horizontal transmission of the transposable element, respectively (Craig, 2002; Parks and Peters, 2009).

Tn7 encodes five genes whose products conduct transposition (Craig et al., 2002). TnsA and TnsB comprise the transposase that catalyzes the DNA breakage and joining reactions at the transposon ends to mobilize the element. TnsC is an AAA regulator protein that activates the transposase when an appropriate target DNA has been found (Stellwagen and Craig, 1998). TnsD and TnsE identify target DNAs and signal TnsABC to activate transposition (Craig, 2002). Target site selection is a prerequisite for activation of transposition with Tn7; transposon excision and insertion does not occur until an appropriate target has been identified. TnsD recognizes a specific site, called its attachment site or *attTn7*, by binding to a highly conserved DNA sequence within the 3′ end of the *glmS* gene. The TnsE protein recognizes an incompletely defined feature associated with discontinuous DNA replication (Peters and Craig, 2001a) that is overrepresented or especially accessible in mobile plasmids, called conjugal plasmids, as they enter a new host cell (Wilkins and Lanka, 1993; Wolkow et al., 1996).

While TnsE-mediated transposition preferentially occurs into mobile plasmids undergoing conjugal DNA replication, the TnsABC+E machinery also recognizes sites within the bacterial chromosome at a lower frequency and with a preference for the region where DNA replication terminates and regions proximal to DNA double-strand breaks (Peters and Craig, 2000; Shi et al., 2008). The orientation of the transposon ends following TnsE-mediated transposition indicates that discontinuously replicated DNA is in some way recognized by TnsE (Peters and Craig, 2001a; Wolkow et al., 1996). As mobile plasmids enter a new host cell, they replicate in a single direction by a discontinuous process, similar to lagging-strand DNA synthesis (Wilkins and Lanka, 1993). In both mobile plasmids and in the chromosome, transposition events occur in a single orientation correlating with the direction of replication progression (Peters and Craig, 2001a, 2001b; Wolkow et al., 1996). It has been shown that TnsE is a DNA binding protein that preferentially binds to DNA structures that present a free 3′-recessed end (Peters and Craig, 2001a). Given that TnsD relies in part on additional host factors in activating transposition (Sharpe and Craig, 1998), it is conceivable that host factors associated

Resource

Cell

Full Dynamic Range Proteome Analysis of *S. cerevisiae* by Targeted Proteomics

Paola Picotti,[1] Bernd Bodenmiller,[1] Lukas N. Mueller,[1] Bruno Domon,[1] and Ruedi Aebersold[1,2,3,4,*]
[1]Institute of Molecular Systems Biology, ETH Zurich, Zurich CH 8093, Switzerland
[2]Competence Center for Systems Physiology and Metabolic Diseases, Zurich CH 8093, Switzerland
[3]Institute for Systems Biology, Seattle, WA 98103, USA
[4]Faculty of Science, University of Zurich, Zurich CH 8057, Switzerland
*Correspondence: aebersold@imsb.biol.ethz.ch
DOI 10.1016/j.cell.2009.05.051

SUMMARY

The rise of systems biology implied a growing demand for highly sensitive techniques for the fast and consistent detection and quantification of target sets of proteins across multiple samples. This is only partly achieved by classical mass spectrometry or affinity-based methods. We applied a targeted proteomics approach based on selected reaction monitoring (SRM) to detect and quantify proteins expressed to a concentration below 50 copies/cell in total *S. cerevisiae* digests. The detection range can be extended to single-digit copies/cell and to proteins undetected by classical methods. We illustrate the power of the technique by the consistent and fast measurement of a network of proteins spanning the entire abundance range over a growth time course of *S. cerevisiae* transiting through a series of metabolic phases. We therefore demonstrate the potential of SRM-based proteomics to provide assays for the measurement of any set of proteins of interest in yeast at high-throughput and quantitative accuracy.

INTRODUCTION

The ability to reliably identify and accurately quantify any protein or set of proteins of interest in a proteome is an essential task in life science research. This has been attempted by two general experimental approaches. The first is based on the generation of affinity reagents exemplified by highly specific antibodies and the development of an array of methods to deploy them for detecting and quantifying specific proteins in complex samples. The second is mass spectrometry (MS)-based quantitative proteomics that attempts to identify and quantify all proteins contained in a sample.

Multiple versions of affinity reagent-based methods (e.g., the broadly used western blot or ELISA approaches) have been implemented. They differ in the type of affinity reagent and detection system used (Uhlen, 2008). The methods with the highest sensitivity have the potential to detect, in principle, low-abundance proteins, with zeptomole detection limits already demonstrated (Pawlak et al., 2002). However, the development of sets of reagents of suitable specificity and affinity to support the conclusive detection and quantification of target protein(s) remains challenging, expensive, and arduous, and coordinated efforts to develop validated affinity reagents are just getting underway (Taussig et al., 2007; Uhlen and Hober, 2009). The methods based on affinity reagents are therefore limited by slow assay development and, usually, also by the inability to significantly multiplex detection of proteins in the same sample.

Similarly to affinity-based methods, a wide range of MS-based proteomic methods have been developed. The most successful of these, in terms of number of proteins identified, use a shotgun strategy in which a subset of peptides present in a tryptic digest of a proteome is selected in an intensity-dependent manner for collision-induced dissociation by a tandem mass spectrometer (Aebersold and Mann, 2003). The resulting fragment ion (MS/MS) spectra are then assigned to sequences in a peptide database and the corresponding peptides and proteins are thus identified. This method provides accurate quantitative data if suitable stable isotope-labeled references are available and included in the analysis (Desiderio and Kai, 1983; Gerber et al., 2003). However, these methods are nontargeted, i.e., in each measurement they stochastically sample a fraction of the proteome that is usually biased toward the higher end of the abundance scale (Domon and Broder, 2004; Picotti et al., 2007). Each repeat analysis required for comparing a proteome at different states will sample only a subset of the proteins it contains and not necessarily the same subset in each repeat, thus precluding the generation of complete and consistent data sets (Wolf-Yadlin et al., 2007). More extensive, although still incomplete and stochastic, proteome coverage can be achieved in large proteome mapping experiments, whereby the proteome is extensively fractionated by multiple approaches and the content of each fraction is sequenced to saturation (Chen et al., 2006; de Godoy et al., 2006, 2008). Such studies carry a significant experimental and computational overhead and are therefore time/labor consuming and can be performed only in highly specialized laboratories. In addition, they mostly retain

Molecular Cell
Short Article

Protein Occupancy Landscape of a Bacterial Genome

Tiffany Vora,[1,2,3] Alison K. Hottes,[1,2] and Saeed Tavazoie[1,2,*]
[1]Department of Molecular Biology
[2]The Lewis-Sigler Institute for Integrative Genomics
Princeton University, Princeton, NJ 08544, USA
[3]Present address: School of Sciences and Engineering, The American University in Cairo, 11835 New Cairo, Egypt
*Correspondence: tavazoie@genomics.princeton.edu
DOI 10.1016/j.molcel.2009.06.035

SUMMARY

Protein-DNA interactions are fundamental to core biological processes, including transcription, DNA replication, and chromosomal organization. We have developed in vivo protein occupancy display (IPOD), a technology that reveals protein occupancy across an entire bacterial chromosome at the resolution of individual binding sites. Application to *Escherichia coli* reveals thousands of protein occupancy peaks, highly enriched within and in close proximity to noncoding regulatory regions. In addition, we discovered extensive (>1 kilobase) protein occupancy domains (EPODs), some of which are localized to highly expressed genes, enriched in RNA-polymerase occupancy. However, the majority are localized to transcriptionally silent loci dominated by conserved hypothetical ORFs. These regions are highly enriched in both predicted and experimentally determined binding sites of nucleoid proteins and exhibit extreme biophysical characteristics such as high intrinsic curvature. Our observations implicate these transcriptionally silent EPODs as the elusive organizing centers, long proposed to topologically isolate chromosomal domains.

INTRODUCTION

Replication, maintenance, and expression of genetic information are processes that are orchestrated through precise interactions of hundreds of proteins with chromosomal DNA. For decades, research has focused on the behavior and functional consequences of DNA-protein interactions at individual loci. However, understanding systems-level behaviors, such as chromosomal organization, genome replication, and transcriptional network dynamics, requires observations at the scale of the entire system. Microarray-based chromatin immunoprecipitation (ChIP-chip) allows global measurements of chromosomal occupancy for individual proteins (Ren et al., 2000). In another global approach, methylase protection, a fraction of all occupied sites are monitored in vivo, independently of the identity of the bound proteins (Tavazoie and Church, 1998). However, there currently exists no comprehensive approach for simultaneous, high-resolution monitoring of all in vivo protein-DNA interactions across the genome. We have developed such a technology and used it to profile protein occupancy of the *E. coli* chromosome at the resolution of individual binding sites.

RESULTS

In Vivo Protein Occupancy Display

In order to globally profile the occupancy of all proteins on chromosomal DNA, we first stabilize in vivo protein-DNA interactions through covalent crosslinking with formaldehyde (Figure 1A). After cell lysis and sonication, protein footprints are minimized to a mode of ~50 bp through DNase I digestion (Figure 1B). Phenol extraction is then used to trap amphipathic protein-DNA complexes at the interface between the organic and aqueous phases. Following interface isolation and crosslink reversal, short DNA fragments are end labeled and hybridized to a high-density tiling array containing 25-mer oligonucleotides at the resolution of one every four base pairs across the entire genome. After scanning and data normalization, a high-resolution global protein occupancy profile is achieved. For each probe on the chip, protein occupancy enrichment or depletion levels are quantified using a z-score that represents the probe-by-probe relative signal intensity with respect to the mean, and normalized to the standard deviation, of signals from replicate hybridizations of whole genomic DNA (Experimental Procedures).

Global Protein Occupancy Profile of the *E. coli* Chromosome

The vast fraction of characterized protein-DNA interactions occur via sequence-specific interactions of transcription factors with DNA within, and in close proximity to, noncoding regulatory regions (Gama-Castro et al., 2008). Consistent with this, we see highly significant occupancy enrichment in noncoding regions as compared to coding regions (Figure 1C). This difference in occupancy is clearly discernable in a local chromosomal view where high-amplitude peaks are largely confined to the regions between genes (Figure 2A). Independent biological replicates demonstrate that the position and relative amplitude of these occupancy peaks show a high level of reproducibility (Figure 2A). Although there is, overall, relative depletion of occupancy within open reading frames (ORFs), occasionally this is interrupted by a sharp occupancy peak (Figures 2A and S1 [available online]). The functional role of these intragenic interactions is not known but could represent a significant gap in our understanding of bacterial gene expression. At high resolution, occupancies of

Cell

Population-Level Transcription Cycles Derive from Stochastic Timing of Single-Cell Transcription

Tatjana Degenhardt,[1,6,7] Katja N. Rybakova,[2,7] Aleksandra Tomaszewska,[1,3] Martijn J. Moné,[2] Hans V. Westerhoff,[2,4] Frank J. Bruggeman,[2,5] and Carsten Carlberg[1,3,*]
[1]Department of Biosciences, University of Kuopio, 70211 Kuopio, Finland
[2]Molecular Cell Physiology, Institute of Molecular Cell Biology, Vrije Universiteit, 1081 HV Amsterdam, The Netherlands
[3]Life Sciences Research Unit, University of Luxembourg, L-1511 Luxembourg, Luxembourg
[4]Manchester Centre for Integrative Systems Biology, Manchester Interdisciplinary Biocentre, University of Manchester, Manchester M1 7ND, UK
[5]Netherlands Institute for Systems Biology, Multiscale Modelling and Nonlinear Dynamics, Centre for Mathematics and Computer Science, Kruislaan 413, 1098SJ Amsterdam, The Netherlands
[6]Present address: Department of Biological Engineering, Massachusetts Institute of Technology, Cambridge, MA 02139, USA
[7]These authors contributed equally to this work
*Correspondence: carsten.carlberg@uni.lu
DOI 10.1016/j.cell.2009.05.029

SUMMARY

Eukaryotic transcription is a dynamic process relying on a large number of proteins. By measuring the cycling expression of the *pyruvate dehydrogenase kinase 4* gene in human cells, we constructed a detailed stochastic model for single-gene transcription at the molecular level using realistic kinetics for diffusion and protein complex dynamics. We observed that gene induction caused an approximate 60 min periodicity of several transcription related processes: first, the covalent histone modifications and presence of many regulatory proteins at the transcription start site; second, RNA polymerase II activity; third, chromatin loop formation; and fourth, mRNA accumulation. Our model can predict the precise timing of single-gene activity leading to transcriptional cycling on the cell population level when we take into account the sequential and irreversible multistep nature of transcriptional initiation. We propose that the cyclic nature of population gene expression is primarily based on the intrinsic periodicity of the transcription process itself.

INTRODUCTION

Eukaryotic transcription is impaired by a repressive chromatin environment of the regulatory regions of genes (Wolffe, 1994). Prior to transcription initiation, several multisubunit protein complexes have to be recruited to these regulatory regions (Cosma, 2002; Narlikar et al., 2002). DNA-binding transcription factors provide the specific link between the regulatory sequences and the large protein complexes. Nuclear receptors (NRs) are a special class of transcription factors that are activated by steroid hormones or nutritional lipids (Chawla et al., 2001). This property allows NRs to directly translate external signals into gene transcription (Carlberg, 1995). In the absence of ligand, most NRs already reside in the nucleus and recruit repressive complexes, including corepressor (CoR) proteins and histone deacetylases (HDACs), to the local chromatin region around their response elements (REs) (Burke and Baniahmad, 2000). Ligand binding results in the dissociation of CoR complexes from the NR proteins and the subsequent recruitment of coactivator (CoA) complexes. Some of these complexes directly affect chromatin structure via histone acetyltransferase activity, while others act as mediators to interact with the basal transcription machinery (Roeder, 2005). ATP-dependent remodeling complexes, containing proteins such as BRG1 and SMARCA2 in their core, support both repression and activation of chromatin regions by increasing the mobility of nucleosomes (Trotter and Archer, 2007). Members of the p160 CoA family, such as RAC3 (Li et al., 1997), and integrator proteins, such as CBP (Chakravarti et al., 1996), covalently modify histone tails. Mediator proteins, like for instance TRAP220, stimulate phosphorylation of the RNA polymerase II (Pol II) at the transcription start site (TSS) (Berk, 1999). This event provokes the exchange of mediator and elongator complexes and allows the start of elongation (Otero et al., 1999). Thus, dozens of proteins with functions that typically rely on protein complex formation are required at both RE and the TSS to commence and complete transcription initiation.

The precise temporal coordination of the mechanisms that govern transcription initiation remains poorly understood. Time-resolved chromatin immunoprecipitation (ChIP) studies that address transcription initiation have been conducted for various NRs, including the androgen receptor (Kang et al., 2002), the thyroid hormone receptor (Sharma and Fondell, 2002), the estrogen receptor (Métivier et al., 2003), and the

Cell

Chromatin Shapes the Mitotic Spindle

Ana Dinarina,[1,4] Céline Pugieux,[1,4] Maria Mora Corral,[1] Martin Loose,[1,5] Joachim Spatz,[2,3] Eric Karsenti,[1] and François Nédélec[1,*]
[1]Cell Biology and Biophysics Unit, European Molecular Biology Laboratory, Heidelberg D-69117, Germany
[2]Department of Biophysical Chemistry, University of Heidelberg, Heidelberg D-69120, Germany
[3]MPI for Metals Research, Heisenbergstr. 3, 70569 Stuttgart, Germany
[4]These authors contributed equally to this work
[5]Present address: Biophysics, BIOTEC, Technische Universität Dresden, Tatzberg 47-51, Dresden 01307, Germany
*Correspondence: nedelec@embl.de
DOI 10.1016/j.cell.2009.05.027

SUMMARY

In animal and plant cells, mitotic chromatin locally generates microtubules that self-organize into a mitotic spindle, and its dimensions and bipolar symmetry are essential for accurate chromosome segregation. By immobilizing microscopic chromatin-coated beads on slide surfaces using a microprinting technique, we have examined the effect of chromatin on the dimensions and symmetry of spindles in *Xenopus laevis* cytoplasmic extracts. While circular spots with diameters around 14–18 μm trigger bipolar spindle formation, larger spots generate an incorrect number of poles. We also examined lines of chromatin with various dimensions. Their length determined the number of poles that formed, with a 6 × 18 μm rectangular patch generating normal spindle morphology. Around longer lines, multiple poles formed and the structures were disorganized. While lines thinner than 10 μm generated symmetric structures, thicker lines induced the formation of asymmetric structures where all microtubules are on the same side of the line. Our results show that chromatin defines spindle shape and orientation.

For a video summary of this article, see the PaperFlick file available with the online Supplemental Data.

INTRODUCTION

The mitotic spindle performs an essential task during eukaryotic cell division: the segregation of sister chromatids. This function implies the establishment of a plane of symmetry, which is materialized by the metaphase plate, orthogonal to the spindle axis and on which the chromosomes are positioned before being separated. During anaphase, chromosomes are segregated by microtubules that bind to sister kinetochores, located on opposite sides of each chromosome. This requires the existence of two overlapping and connected arrays of antiparallel microtubules, capable of resisting inward directed forces produced by the pulling forces of the kinetochore microtubules.

Two pathways of spindle assembly have been identified, the centrosomal and the chromatin pathway (Walczak and Heald, 2008). They are independent and complementary and cells may rely on one or both pathways to assemble a spindle. For example, two centrosomes and kinetochore pairs positioned back-to-back on sister chromatids may be sufficient to form a spindle in the small yeast cell (Winey et al., 1995). In contrast, in large cytoplasmic volumes such as in *Xenopus laevis* egg extracts, spindles can assemble in the absence of kinetochores and centrosomes (Heald et al., 1996). In this system, microtubules are generated near chromatin and organized into a bipolar spindle by associated proteins, hence the term "chromatin pathway" (also known as acentrosomal). Understanding this pathway is of major importance because it is found in higher eukaryotes, including frogs, green monkeys (Khodjakov et al., 2000), *Drosophila* S2 cells (Goshima et al., 2008; Mahoney et al., 2006), *Drosophila* oocytes (Matthies et al., 1996), mouse oocytes (Schuh and Ellenberg, 2007), human cells (Bird and Hyman, 2008), and plants (Lloyd and Chan, 2006).

Although the enzymatic mechanism by which the chromatin pathway controls local microtubule growth has been partly resolved (Walczak and Heald, 2008), the overall effects of chromatin on spindle size and symmetry properties have not been examined. This issue has been addressed using spindles assembled around artificial chromosomes in *X. laevis* egg extracts, but there was no method to create chromatin in a defined shape. The other challenge was to obtain statistically meaningful data on the relationship between chromatin mass and spindle properties. Only one study has examined the effect of chromatin geometry on spindle morphology (Gaetz et al., 2006), but the method was limited in the variety of chromatin patterns that could be tested.

We have devised a new method to control both the size and geometry of chromatin patterns and to study their impact on the morphology of mitotic spindles. We were also able to capture time-lapse movies of spindle assembly, including the initial nucleation phase. We found that chromatin size and geometry play a fundamental role in the determination of spindle size and define the characteristic symmetries of the structure.

RESULTS

Spindles Self-Organize on Chromatin-Coated Immobilized Beads

It has long been known that large DNA plasmids (about 10 kb or more) could trigger spindle assembly when injected into *X. laevis* eggs (Karsenti et al., 1984). However, the exact quantity of chromatin required to make a spindle remained unknown. For

Cell

Theory

Defining Network Topologies that Can Achieve Biochemical Adaptation

Wenzhe Ma,[1,2,3] Ala Trusina,[2,3] Hana El-Samad,[2,4] Wendell A. Lim,[2,5,*] and Chao Tang[1,2,3,4,*]
[1]Center for Theoretical Biology, Peking University, Beijing 100871, China
[2]California Institute for Quantitative Biosciences
[3]Department of Bioengineering and Therapeutic Sciences
[4]Department of Biochemistry and Biophysics
[5]Howard Hughes Medical Institute and Department of Cellular and Molecular Pharmacology
University of California, San Francisco, CA 94158, USA
*Correspondence: lim@cmp.ucsf.edu (W.A.L.), chao.tang@ucsf.edu (C.T.)
DOI 10.1016/j.cell.2009.06.013

SUMMARY

Many signaling systems show adaptation—the ability to reset themselves after responding to a stimulus. We computationally searched all possible three-node enzyme network topologies to identify those that could perform adaptation. Only two major core topologies emerge as robust solutions: a negative feedback loop with a buffering node and an incoherent feedforward loop with a proportioner node. Minimal circuits containing these topologies are, within proper regions of parameter space, sufficient to achieve adaptation. More complex circuits that robustly perform adaptation all contain at least one of these topologies at their core. This analysis yields a design table highlighting a finite set of adaptive circuits. Despite the diversity of possible biochemical networks, it may be common to find that only a finite set of core topologies can execute a particular function. These design rules provide a framework for functionally classifying complex natural networks and a manual for engineering networks.

For a video summary of this article, see the PaperFlick file with the Supplemental Data available online.

INTRODUCTION

The field of systems biology is largely focused on mapping and dissecting cellular networks with the goal of understanding how complex biological behaviors arise. Extracting general design principles—the rules that underlie what networks can achieve particular biological functions—remains a challenging task, given the complexity of cellular networks and the small fraction of existing networks that have been well characterized. Nonetheless, growing evidence suggests the existence of design principles that unify the organization of diverse circuits across all organisms. For example, it has been shown that there are recurrent network motifs linked to particular functions, such as temporal expression programs (Shen-Orr et al., 2002), reliable cell decisions (Brandman et al., 2005), and robust and tunable biological oscillations (Tsai et al., 2008).

These findings suggest an intriguing hypothesis: despite the apparent complexity of cellular networks, there might only be a limited number of network topologies that are capable of robustly executing any particular biological function. Some topologies may be more favorable because of fewer parameter constraints. Other topologies may be incompatible with a particular function. Although the precise implementation could differ dramatically in different biological systems, depending on biochemical details and evolutionary history, the same core set of network topologies might underlie functionally related cellular behaviors (Milo et al., 2002; Wagner, 2005; Ma et al., 2006; Hornung and Barkai, 2008). If this hypothesis is correct, then one may be able to construct a unified function-topology mapping that captures the essential barebones topologies underpinning the function. Such core topologies may otherwise be obscured by the details of any specific pathway and organism. Such a map would help organize our ever-expanding database of biological networks by functionally classifying key motifs in a network. Such a map might also suggest ways to therapeutically modulate a system. A circuit function-topology map would also be invaluable for synthetic biology, providing a manual for how to robustly engineer biological circuits that carry out a target function.

To investigate this hypothesis, we have computationally explored the full range of simple enzyme circuit architectures that are capable of executing one critical and ubiquitous biological behavior—adaptation. We ask if there are finite solutions for achieving adaptation. Adaptation refers to the system's ability to respond to a change in input stimulus then return to its prestimulated output level, even when the change in input persists. Adaptation is commonly used in sensory and other signaling networks to expand the input range that a circuit is able to sense, to more accurately detect changes in the input, and to maintain homeostasis in the presence of perturbations. A mathematical description of adaptation is diagrammed in Figure 1A, in which two characteristic quantities are defined: the circuit's sensitivity to input change and the precision of adaptation. If the system's response returns exactly to the prestimulus level (infinite precision), it is called the perfect adaptation. Examples of perfect or near perfect adaptation range from the chemotaxis of bacteria (Berg

PERSPECTIVE

The Systems Biology Graphical Notation

Nicolas Le Novère[1], Michael Hucka[2], Huaiyu Mi[3], Stuart Moodie[4], Falk Schreiber[5,6], Anatoly Sorokin[7], Emek Demir[8], Katja Wegner[9], Mirit I Aladjem[10], Sarala M Wimalaratne[11], Frank T Bergman[12], Ralph Gauges[13], Peter Ghazal[4,14], Hideya Kawaji[15], Lu Li[1], Yukiko Matsuoka[16], Alice Villéger[17,18], Sarah E Boyd[19], Laurence Calzone[20], Melanie Courtot[21], Ugur Dogrusoz[22], Tom C Freeman[14,23], Akira Funahashi[24], Samik Ghosh[16], Akiya Jouraku[24], Sohyoung Kim[10], Fedor Kolpakov[25,26], Augustin Luna[10], Sven Sahle[13], Esther Schmidt[1], Steven Watterson[4,22], Guanming Wu[27], Igor Goryanin[4], Douglas B Kell[18,28], Chris Sander[8], Herbert Sauro[12], Jacky L Snoep[29], Kurt Kohn[10] & Hiroaki Kitano[16,30,31]

Circuit diagrams and Unified Modeling Language diagrams are just two examples of standard visual languages that help accelerate work by promoting regularity, removing ambiguity and enabling software tool support for communication of complex information. Ironically, despite having one of the highest ratios of graphical to textual information, biology still lacks standard graphical notations. The recent deluge of biological knowledge makes addressing this deficit a pressing concern. Toward this goal, we present the Systems Biology Graphical Notation (SBGN), a visual language developed by a community of biochemists, modelers and computer scientists. SBGN consists of three complementary languages: process diagram, entity relationship diagram and activity flow diagram. Together they enable scientists to represent networks of biochemical interactions in a standard, unambiguous way. We believe that SBGN will foster efficient and accurate representation, visualization, storage, exchange and reuse of information on all kinds of biological knowledge, from gene regulation, to metabolism, to cellular signaling.

"Un bon croquis vaut mieux qu'un long discours" ("A good sketch is better than a long speech"), said Napoleon Bonaparte. This claim is nowhere as true as for technical illustrations. Diagrams naturally engage innate cognitive faculties[1] that humans have possessed since before the time of our cave-drawing ancestors. Little wonder that we find ourselves turning to them in every field of endeavor. Just as with written human languages, communication involving diagrams requires that authors and readers agree on symbols, the rules for arranging them and the interpretation of the results. The establishment and widespread use of standard notations have permitted many fields to thrive. One can hardly imagine today's electronics industry, with its powerful, visually oriented design and automation tools, without having first established standard notations for circuit diagrams. Such was not the case in biology[2]. Despite the visual nature of much of the information exchange, the field was permeated with *ad hoc* graphical notations having little in common between different researchers, publications, textbooks and software tools. No standard visual language existed for describing biochemical interaction networks, inter- and intracellular signaling gene regulation—concepts at the core of much of today's research in molecular, systems and synthetic biology. The closest to a standard is the notation long used in many metabolic and signaling pathway maps, but in reality, even that lacks uniformity between sources and suffers from undesirable ambiguities (Fig. 1). Moreover, the existing tentative representations, however well crafted, were ambiguous, and only suitable for specific needs, such as representing metabolic networks or signaling pathways or gene regulation.

The molecular biology era, and more recently the rise of genomics and other high-throughput technologies, have brought a staggering increase in data to be interpreted. It also favored the routine use of software to help formulate hypotheses, design experiments and interpret results. As a group of biochemists, modelers and computer scientists working in systems biology, we believe establishing standard graphical notations is an important step toward more efficient and accurate transmission of biological knowledge among our different communities. Toward this goal, we initiated the SBGN project in 2005, with the aim of developing and standardizing a systematic and unambiguous graphical notation for applications in molecular and systems biology.

Historical antecedents

Graphical representation of biochemical and cellular processes has been used in biochemical textbooks as far back as sixty years ago[3], reaching an apex in the wall charts hand drawn by Nicholson[4] and Michal[5]. Those graphs describe the processes that transform a set of inputs into a set of outputs, in effect being process, or state transition, diagrams. This style was emulated in the first database systems that depicted metabolic networks, including EMP[6], EcoCyc[7] and KEGG[8]. More notations have been 'defined' by virtue of their implementation in specialized software tools such as pathway and network designers (e.g., NetBuilder[9], Patika[10], JDesigner[11], CellDesigner[12]). Those

A list of affiliations appears at the end of the paper.

Published online 7 August 2009; doi:10.1038/nbt1558

The EMBO Journal (2009) 28, 2209–2219 | © 2009 European Molecular Biology Organization | All Rights Reserved 0261-4189/09
www.embojournal.org

THE EMBO JOURNAL

Increased RNA polymerase availability directs resources towards growth at the expense of maintenance

Bertil Gummesson[1], Lisa U Magnusson[1,*], Martin Lovmar[2], Kristian Kvint, Örjan Persson, Manuel Ballesteros[3], Anne Farewell and Thomas Nyström*

Department of Cell and Molecular Biology, Gothenburg University, Göteborg, Sweden

Nutritionally induced changes in RNA polymerase availability have been hypothesized to be an evolutionary primeval mechanism for regulation of gene expression and several contrasting models have been proposed to explain how such 'passive' regulation might occur. We demonstrate here that ectopically elevating *Escherichia coli* RNA polymerase ($E\sigma^{70}$) levels causes an increased expression and promoter occupancy of ribosomal genes at the expense of stress-defense genes and amino acid biosynthetic operons. Phenotypically, cells overproducing $E\sigma^{70}$ favours growth and reproduction at the expense of motility and damage protection; a response reminiscent of cells with no or diminished levels of the alarmone guanosine tetraphosphate (ppGpp). Consistently, we show that cells lacking ppGpp displayed markedly elevated levels of free $E\sigma^{70}$ compared with wild-type cells and that the repression of ribosomal RNA expression and reduced growth rate of mutants with constitutively elevated levels of ppGpp can be suppressed by overproducing $E\sigma^{70}$. We conclude that ppGpp modulates the levels of free $E\sigma^{70}$ and that this is an integral part of the alarmone's means of regulating a trade-off between growth and maintenance.

The EMBO Journal (2009) **28,** 2209–2219. doi:10.1038/emboj.2009.181; Published online 2 July 2009
Subject Categories: chromatin & transcription
Keywords: passive regulation; ppGpp; RNA polymerase; stringent control; transcriptional trade-off

Introduction

The most pervasive means of altering the relative abundance of transcripts in the cell is to control the efficiency at which the RNA polymerase initiates transcription at different promoters. In *Escherichia coli*, RNA polymerase consists of the core enzyme (E) containing the $\alpha_2\beta\beta'\omega$ subunits, and one of the seven possible sigma (σ) factors conferring promoter specificity to E by making sequence-specific contacts to DNA (Gross *et al*, 1992). The majority of genes (housekeeping genes) expressed during exponential growth of *E. coli* require σ^{70} (encoded by *rpoD*) for transcription initiation. This sigma factor directs E to genes encoding proliferation-related activities, including the genes of the protein synthesizing system (PSS; i.e. those encoding the ribosomes, tRNAs and factors required for translation). In addition, a large number of maintenance and stress-defense genes induced upon growth limitations are also dependent on the $E\sigma^{70}$ holoenzyme. Directing $E\sigma^{70}$ to appropriate promoters (or inhibiting promoter contacts) under changing conditions is to a large part accomplished by specific activators and repressors. However, $E\sigma^{70}$-dependent genes have been argued to be subjected to differential control also by changes in $E\sigma^{70}$ availability, a so-called passive regulation of gene expression.

Ole Maaløe was perhaps first in presenting a model for passive control of gene expression inspired by the conviction that the massive alterations of gene expression needed during drastically changing growth conditions, such as nutrient limitations, required a more robust control than those afforded by specific repression, de-repression, and activator circuits (Maaløe, 1979). This type of gene regulation might have been operational before the evolution of specific regulatory factors and maintained some of its importance in representing a regulatory baseline control on top of which more specific and pronounced effects can be achieved with activators and repressors. Maaløe suggested, for example, that the synthesis of the PSS is regulated by $E\sigma^{70}$ availability, which changes with changing growth conditions (Bremer and Dennis, 1996). Although details of Maaløe's original model has been found wanting, the assumption that individual promoters compete with each other for a limiting amount of free $E\sigma^{70}$ has been confirmed (Shepherd *et al*, 2001; Jishage *et al*, 2002; Bremer *et al*, 2003; Magnusson *et al*, 2003; Grigorova *et al*, 2006).

Several authors have presented updated models for passive regulation and endorsed passive control as an integral part of stringent control by the nucleotide guanosine tetraphosphate (ppGpp). Cells of *E. coli* elicit a swift down-regulation of the PSS during amino acid starvation—a response called the stringent response—and ppGpp, acting together with the protein DksA, is the effector molecule of this response (reviewed in Potrykus and Cashel, 2008). The nucleotide ppGpp is produced by RelA and/or SpoT. This occurs not only in response to amino acid limitation but also upon starvation for many different kinds of nutrients and in circumstances restricting growth (Cashel *et al*, 1996). A key feature in one passive model of gene regulation, referred to

*Corresponding authors. LU Magnusson or T Nystrom, Department of Cell and Molecular Biology, Gothenburg University, Medicinaregatan 9C, Göteborg 41390, Sweden. Tel.: +46 31 786 2590; +46 31 786 2582; Fax: +46 31 786 2599; E-mails: thomas.nystrom@cmb.gu.se or lisa.magnusson@cmb.gu.se
[1]These authors contributed equally to this work
[2]Present address: Astra Tech AB, Mölndal, Sweden
[3]Present address: Universidad Pablo de Olavide, Seville, Spain

Received: 15 January 2009; accepted: 5 June 2009; published online: 2 July 2009

A Publication of The Genetics Society of America

GENETICS

Originally published as *Genetics* Published Articles Ahead of Print on May 27, 2009.

Genetics, Vol. 182, 1159-1164, August 2009, Copyright © 2009
doi:10.1534/genetics.109.103333

Evolution of Stochastic Switching Rates in Asymmetric Fitness Landscapes

Marcel Salathé[1], Jeremy Van Cleve and Marcus W. Feldman

Department of Biological Sciences, Stanford University, Stanford, California 94305-5020

[1] *Corresponding author:* Department of Biology, Stanford University, Stanford, CA 94305-5020.
E-mail: salathe@stanford.edu

Uncertain environments pose a tremendous challenge to populations: The selective pressures imposed by the environment can change so rapidly that adaptation by mutation alone would be too slow. One solution to this problem is given by the phenomenon of stochastic phenotype switching, which causes genetically uniform populations to be phenotypically heterogenous. Stochastic phenotype switching has been observed in numerous microbial species and is generally assumed to be an adaptive bet-hedging strategy to anticipate future environmental change. We use an explicit population genetic model to investigate the evolutionary dynamics of phenotypic switching rates. We find that whether or not stochastic switching is an adaptive strategy is highly contingent upon the fitness landscape given by the changing environment. Unless selection is very strong, asymmetric fitness landscapes—where the cost of being maladapted is not identical in all environments—strongly select against stochastic switching. We further observe a threshold phenomenon that causes switching rates to be either relatively high or completely absent, but rarely intermediate. Our finding that marginal changes in selection pressures can cause fundamentally different evolutionary outcomes is important in a wide range of fields concerned with microbial bet hedging.

THIS ARTICLE
Full Text
Full Text (PDF)
All Versions of this Article:
genetics.109.103333v1
genetics.109.103333v2
182/4/1159 *most recent*
Alert me when this article is cited
Alert me if a correction is posted

SERVICES
Email this article to a friend
Similar articles in this journal
Similar articles in PubMed
Alert me to new issues of the journal
Download to citation manager
Reprints & Permissions

GOOGLE SCHOLAR
Articles by Salathé, M.
Articles by Feldman, M. W.

PUBMED
PubMed Citation
Articles by Salathé, M.
Articles by Feldman, M. W.

Online ISSN: 1943-2361 Print ISSN: 0016-6731

phone: 412-268-1812 fax: 412-268-1813 email: genetics-gsa@andrew.cmu.edu

GSA A Publication of The Genetics Society of America

GENETICS

Originally published as *Genetics* Published Articles Ahead of Print on May 4, 2009.

Genetics, Vol. 182, 845-850, July 2009, Copyright © 2009
doi:10.1534/genetics.109.102798

Epigenetic Inheritance and the Missing Heritability Problem

Montgomery Slatkin[1]

Department of Integrative Biology, University of California, Berkeley, California 94720-3140

[1] *Author e-mail:* slatkin@berkeley.edu

Epigenetic phenomena, and in particular heritable epigenetic changes, or transgenerational effects, are the subject of much discussion in the current literature. This article presents a model of transgenerational epigenetic inheritance and explores the effect of epigenetic inheritance on the risk and recurrence risk of a complex disease. The model assumes that epigenetic modifications of the genome are gained and lost at specified rates and that each modification contributes multiplicatively to disease risk. The potentially high rate of loss of epigenetic modifications causes the probability of identity in state in close relatives to be smaller than is implied by their relatedness. As a consequence, the recurrence risk to close relatives is reduced. Although epigenetic modifications may contribute substantially to average risk, they will not contribute much to recurrence risk and heritability unless they persist on average for many generations. If they do persist for long times, they are equivalent to mutations and hence are likely to be in linkage disequilibrium with SNPs surveyed in genomewide association studies. Thus epigenetic modifications are a potential solution to the problem of missing causality of complex diseases but not to the problem of missing heritability. The model highlights the need for empirical estimates of the persistence times of heritable epialleles.

THIS ARTICLE
Full Text
Full Text (PDF)
All Versions of this Article:
genetics.109.102798v1
182/3/845 *most recent*
Alert me when this article is cited
Alert me if a correction is posted

SERVICES
Email this article to a friend
Related articles in Genetics
Similar articles in this journal
Similar articles in PubMed
Alert me to new issues of the journal
Download to citation manager
Reprints & Permissions

CITING ARTICLES
Citing Articles via HighWire

GOOGLE SCHOLAR
Articles by Slatkin, M.

PUBMED
PubMed Citation
Articles by Slatkin, M.

Related articles in Genetics:

ISSUE HIGHLIGHTS

Genetics 2009 182: NP. [Full Text]

This article has been cited by other articles:

GENETICS HOME

A. E. Handel and S. V. Ramagopalan
Public Health Implications of Epigenetics
Genetics, August 1, 2009; 182(4): 1397 - 1398.
[Full Text] [PDF]

Online ISSN: 1943-2361 Print ISSN: 0016-6731

phone: 412-268-1812 fax: 412-268-1813 email: genetics-gsa@andrew.cmu.edu

J|A|C|S
COMMUNICATIONS

Published on Web 08/06/2009

Autonomously Oscillating Viscosity in Microgel Dispersions

Daisuke Suzuki,*,† Hajime Taniguchi,‡ and Ryo Yoshida*,‡,§

International Young Researchers Empowerment Center, Shinshu University, 3-15-1 Tokida, Ueda, Nagano 386-8567, Japan, Department of Materials Engineering, Graduate School of Engineering, The University of Tokyo, 7-3-1 Hongo, Bunkyo-ku, Tokyo 113-8656, Japan, and PRESTO, Japan Science and Technology Agency, 4-1-8 Honcho, Kawaguchi, Saitama, Japan

Received June 9, 2009; E-mail: d_suzuki@shinshu-u.ac.jp; ryo@cross.t.u-tokyo.ac.jp

Rheological properties of colloidal dispersions are widely studied because such dispersions are important in many applications, such as paints, cosmetics, food, and pharmaceutical formulations. In this field, polymer colloids are attractive because they can be synthesized in uniform sizes and surface properties. Also, the sizes and properties can be controlled and reproduced as a result of contributions by many researchers over a long period of time.[1] In particular, over the past decade or so, there has been increasing interest in aqueous stimuli-responsive microgels because of their multiple functions that may be applied in various applications, including drug delivery,[2] photonic crystals,[3] chemical/biological separation,[4] templating for inorganic nanoparticle synthesis,[5] emulsifiers,[6] and rheological modifiers.[7]

In contrast to simple stimuli-sensitive microgels such as temperature- and pH-sensitive ones, very recently we reported *self-oscillating* microgels.[8] Our microgels show an autonomous *swelling/deswelling* oscillation that is synchronized with the redox oscillation of the Belousov–Zhabotinsky (BZ) reaction.[9] The microgels are copolymerized with the tris(2,2′-bipyridine)ruthenium monomer, denoted $Ru(bpy)_3$, which is the catalyst for the BZ reaction. Thus, the volume of the microgel oscillates in aqueous solution containing the substrates for the BZ reaction. In addition, an autonomous *flocculation/redispersion* oscillation near the volume phase transition temperature of the microgels was discovered.[10] In general, the viscosity is related to the effective volume fraction of the microgels and the status of dispersion (flocculated or not). Thus, these two types of autonomous oscillation of the microgels should affect the viscosity in the dispersion. If autonomously oscillating viscosity of the dispersion is realized, this technology could be applied in many applications, as have electro- and magnetorheological (ER and MR) fluids. In particular, the dispersion with autonomously oscillating viscosity may be used as a micropump, which could realize next-generation microfluidics devices.

In this communication, we demonstrate a new rheological property of colloidal dispersions using self-oscillating microgels, which were synthesized by surfactant-free aqueous precipitation polymerization as in our previous report.[8] The chemical structure of the microgel is shown in SI Figure 1 in the Supporting Information. Our previous study revealed that the microgels obtained by this approach are very monodispersed.[8] In this case, dynamic light scattering (DLS) measurements gave a hydrodynamic diameter of ~200 nm for the obtained microgel in a dilute dispersion (at 25 °C in 1 mM NaCl solution). Before the self-oscillating study, we checked the temperature dependence of the hydrodynamic diameters of the reduced Ru(II) and oxidized Ru(III) states by DLS. From these data, we can estimate the degree of volume change in the oscillation. In this case, the diameters were measured to be several tens of nanometers at all temperatures (see SI Figure 2).

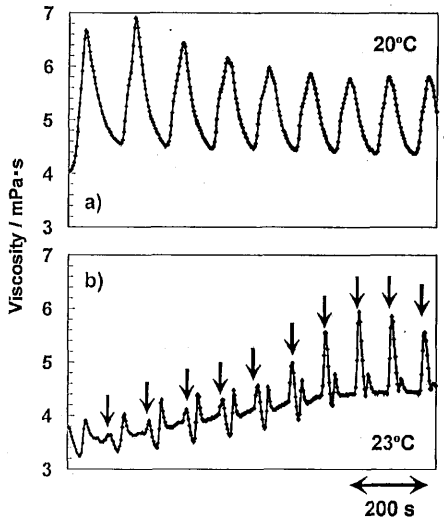

Figure 1. Self-oscillating profiles of viscosity in the microgel dispersions. The microgels were dispersed in aqueous solution containing MA (100 mM), $NaBrO_3$ (150 mM), and HNO_3 (0.5 M). The microgel concentration was 5 wt %. All of the data were taken at a constant shear rate of 132 s^{-1}. The viscosity was measured at various temperatures; (a) 20 and (b) 23 °C. Characteristic peaks that emerged at 23 °C are indicated by the arrows in (b).

Next, we carried out the BZ reaction using the microgel dispersions. Malonic acid (MA), sodium bromate ($NaBrO_3$), and HNO_3 were used as substrates for the BZ reaction at a fixed concentration. Figure 1 shows self-oscillating profiles of viscosity in microgel dispersions measured at different temperatures. Because one of the components of the microgel, poly(*N*-isopropylacrylamide) (pNIPAm),[11] shows a temperature-sensitive property, the diameter of the microgel decreased as the temperature increased up to the critical flocculation temperature (CFT) (see SI Figure 2). In this case, concentrations of microgel (5 wt %) and substrates for the BZ reaction were fixed.[12] Thus, the effective volume fraction of the microgels should decrease with increasing temperature up to the CFT. At 20 °C (Figure 1a), autonomously oscillating viscosity was observed. The waveform of the oscillation is similar to that detected by optical transmittance as reported previously.[8] With increasing temperature, oscillating profiles with the same waveform but decreased amplitude were observed up to 22 °C (see SI Figure 3a). The decrease in amplitude is attributed to the decrease in effective volume fraction of the microgels at higher temperatures.[13] Next, the waveform suddenly changed at 23 °C to include two peaks per period (Figure 1b). Finally, oscillation was no longer

† Shinshu University.
‡ The University of Tokyo.
§ PRESTO.

10.1021/ja904677g CCC: $40.75

J|A|C|S COMMUNICATIONS

Published on Web 08/07/2009

Strand Invasion of Extended, Mixed-Sequence B-DNA by γPNAs

Gaofei He, Srinivas Rapireddy, Raman Bahal, Bichismita Sahu, and Danith H. Ly*

Department of Chemistry and Center for Nucleic Acids Science and Technology (CNAST), Carnegie Mellon University, 4400 Fifth Avenue, Pittsburgh, Pennsylvania 15213

Received January 12, 2009; E-mail: dly@andrew.cmu.edu

Peptide nucleic acids (PNAs) are a promising class of nucleic acid mimics developed in the last two decades in which the naturally occurring sugar phosphodiester backbone has been replaced by achiral *N*-(2-aminoethyl)glycine units (Scheme 1A).[1] In addition to their ability in hybridizing to cDNA or RNA strands, PNAs can invade double-stranded DNA.[2] Strand invasion occurs predominantly in two modes, depending on the target sequence: through Watson−Crick base pairing to form a 1:1 PNA/DNA complex[3] or in combination with Hoogsteen base pairing to form a 2:1 complex.[4] The simplicity and generality of their recognition along with the ease and flexibility of their synthesis make PNAs an attractive class of antigene reagents. However, with the current design, not every sequence can be accessed by PNAs; in particular, those that contain all four nucleobases are not accessible. Mixed-sequence PNAs have been shown to be capable of invading supercoiled plasmid DNA[5−7] and certain regions of genomic DNA,[8] but they are not capable of invading intact, linear double-helical B-form DNA (B-DNA). Recently, two approaches, "tail-clamp"[9,10] and "double-duplex"[11] invasion, that enable mixed-sequence PNAs to invade B-DNA have been developed. However, they are not without limitations. The first approach still requires a stretch of homopurine target for anchoring triplex binding, while the second, although more relaxed in sequence selection, requires an elaborate nucleobase substitution and the need to use two strands of PNAs to invade B-DNA, complicating their design and greatly limiting their utility.[12] In this communication, we show that mixed-sequence PNAs with lengths of 15−20 nucleotides (nt), when preorganized into a right-handed helix, can invade double-helical B-DNA. Strand invasion occurs in a sequence-specific manner through direct Watson−Crick base pairing. In this case, only a single strand of γPNA is required for invasion, and no nucleobase substitution is needed.

Recently, we showed that PNAs, which as individual strands do not have well-defined conformations, can be preorganized into a right-handed helix by installing an (*S*)-Me stereogenic center at the γ-backbone position (Scheme 1A).[13] These helical γPNAs exhibit strong binding affinity for cDNA and RNA strands. As decamers, mixed-sequence γPNAs are unable to invade B-DNA, but strand invasion can be rescued by appending an acridine moiety (DNA intercalator) to one of the termini[13] or by replacing a cytosine nucleobase with an energetically more favorable synthetic analogue.[14] These results suggest that the binding free energies of the decameric γPNAs are already near the invasion threshold and that not much more is needed to enable them to invade B-DNA. On the basis of these findings, we speculated that as an alternative to the aforementioned strategies, the required binding free energy may also be attained by extending the size of the γPNA oligomers, since a γPNA−DNA duplex is generally thermodynamically more stable than a DNA−DNA duplex. If this design strategy could be achieved, it would not only circumvent the need to attach ancillary agents to PNAs, which may compromise their recognition specificity and complicate their synthesis, but also allow γPNAs to recognize extended DNA targets, which has been a goal of antigene design.[2,15,16] To test this hypothesis, we synthesized a series of γPNA oligomers with various sizes (Scheme 1B) that were designed to bind to both the top and bottom strands of the DNA target and then assessed their invasion capability using a combination of gel-shift, enzymatic, and chemical-probing assays.

Scheme 1. (A) Chemical Structures of PNA and γPNA and (B) Sequence of γPNAs and a Selected Region of the DNA Target

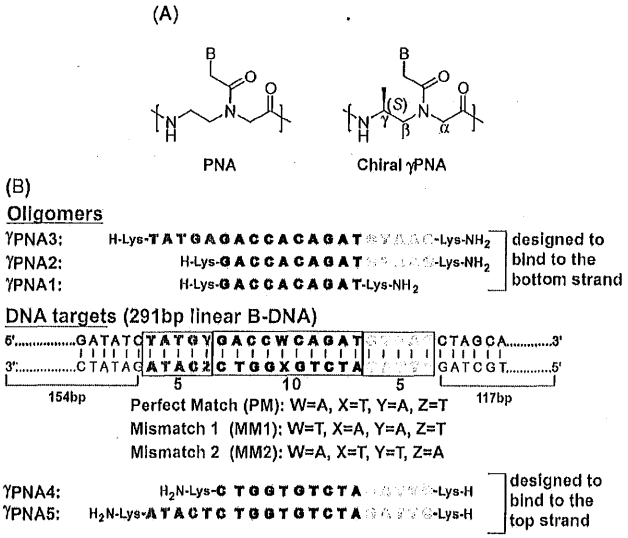

The gel-shift assay was performed by incubation of a 291 base pair (bp) PCR fragment containing a perfect-match (**PM**) binding site with different concentrations of **γPNA1−3** in 10 mM sodium phosphate (NaPi) buffer at 37 °C for 16 h, followed by gel separation and SYBR Gold staining. Consistent with our earlier result,[13] we observed no binding of **γPNA1**, a decamer, at γPNA/DNA ratios as high as 20:1 (Figure 1A, lanes 3 and 4). However, in the case of 15-mer **γPNA2** and 20-mer **γPNA3**, we noticed the appearance of a shifted band (lanes 5, 6, 8 and 9). The intensity of the new band gradually increased with increasing γPNA concentration, and the mobility decreased with increasing oligomer length. Formation of this complex appeared to be more efficient with **γPNA3** than with **γPNA2**, as reflected in the ratio of the bound-to-unbound DNA (compare lanes 8 with 5 and lanes 9 with 6). This is expected, since **γPNA3** should form a thermodynamically more stable complex with DNA as a result of its greater length. Binding appeared to be unique to γPNAs and occurred in a sequence-specific manner: neither incubation of DNA containing the **PM** binding site with PNAs having identical nucleobase sequences (PNA2, lane 7; PNA3, lane 10) nor incubation of DNA having a single-base mismatch in the middle (**MM1**) or toward one end (**MM2**) of the binding site with γPNAs resulted in formation of any shifted bands (Figure 1B, lanes 4−9). Similar findings were

10.1021/ja900228j CCC: $40.75

J|A|C|S COMMUNICATIONS

Published on Web 08/24/2009

Genetic Incorporation of a Small, Environmentally Sensitive, Fluorescent Probe into Proteins in *Saccharomyces cerevisiae*

Hyun Soo Lee, Jiantao Guo, Edward A. Lemke, Romerson D. Dimla, and Peter G. Schultz*

Department of Chemistry and the Skaggs Institute for Chemical Biology, The Scripps Research Institute, 10550 North Torrey Pines Road, La Jolla, California 92037

Received June 15, 2009; E-mail: schultz@scripps.edu

The introduction of fluorescent probes into proteins provides a powerful tool to study protein structure and function either in vitro or in vivo.[1] One particularly useful method involves genetically fusing the protein of interest to fluorescent proteins.[2] However, the size of naturally occurring fluorescent proteins (>20 kDa) and the typical requirement for C- or N-terminal fusions limit their utility as a local probe of structure and in some cases can perturb the structure or function of a protein. A variety of other methods have been developed to introduce fluorescent probes into protein in vitro and in vivo including the selective chemical[3] or enzymatic[4] modification of specific recognition motifs, the use of intein-based semisynthetic methods,[5] and in vitro protein translation[6] with chemically aminoacylated tRNAs. Although very useful, each approach has its own limitations including protein size and yields, modifications to the native protein sequence, or reagents/protocols that are not compatible with live cells. To augment and extend these methods, we have attempted to genetically encode small, fluorescent amino acids directly in living cells.[7] In this study, we report the site-specific incorporation of an environmentally sensitive, fluorescent amino acid into proteins in response to the amber nonsense codon (TAG) with good yield and high fidelity in yeast. We demonstrate that the method can be used as a local probe of conformational changes in protein structure induced by ligand binding.

6-Propionyl-2-(*N*,*N*-dimethyl)aminonaphthalene, prodan,[8] is a highly environmentally sensitive fluorophore that is widely used in biochemistry and cell biology.[9] To genetically encode the amino acid analogue of prodan, 3-(6-acetylnaphthalen-2-ylamino)-2-aminopropanoic acid (Anap, **1**), it was synthesized in six steps starting with 1-(6-hydroxynaphthalen-2-yl)ethanone (Figure S1, Supporting Information). The extinction coefficient (17 500 cm^{-1} M^{-1}) and quantum yield (0.48, Figure S2, Supporting Information) of Anap in EtOH (360 nm) are comparable to those of prodan (18 400 $cm^{-1}M^{-1}$ and 0.71).[8,10] The fluorescence spectra in various solvents also exhibit sensitivity to solvent polarity similar to other prodan probes with a significant shift in emission maximum (λ_{em}^{max}) on transitioning from water (λ_{em}^{max} = 490 nm) to ethyl acetate (λ_{em}^{max} = 420 nm) (Figure 1). Compared with dansyl- or coumarin-containing amino acids, Anap has enhanced environmental sensitivity with comparable or increased brightness.[9c,11]

To genetically encode this amino acid in *Saccharomyces cerevisiae*, an orthogonal *Escherichia coli* amber suppressor tRNA/leucyl-tRNA synthetase ($tRNA_{CUA}^{Leu}$/LeuRS) pair[12] was used on the basis of previous experiments[7a,13] which showed that LeuRS mutants can accommodate unnatural amino acids with large hydrophobic side chains. To alter the specificity of LeuRS so that it aminoacylates $tRNA_{CUA}^{Leu}$ with Anap and no endogenous amino acids, a LeuRS library was constructed by randomizing five residues

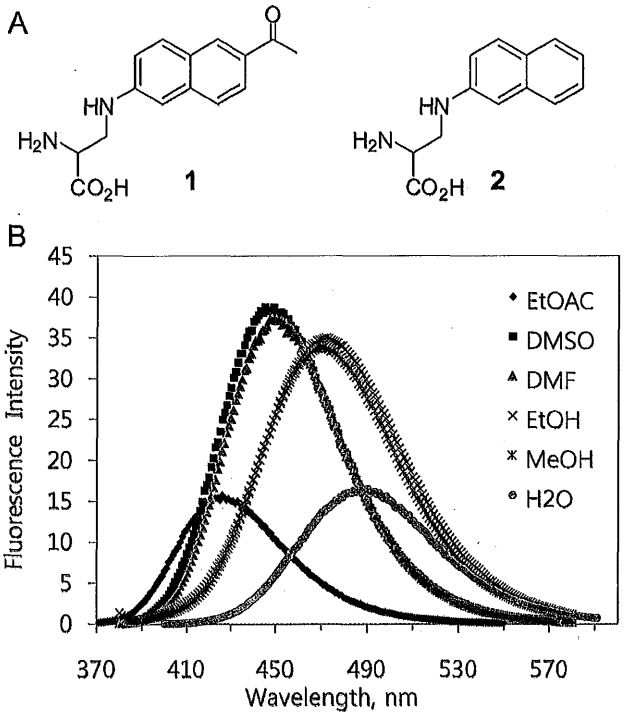

Figure 1. (a) Chemical structures of Anap (**1**) and Nap (**2**). (b) Fluorescence spectra of **1** in various solvents; samples were excited at 350 nm.

(M40, L41, Y499, Y527, and H537) in the leucine-binding site.[7a,12] The library was then subjected to rounds of alternating positive and negative selections as previously described,[14] but unfortunately no mutant LeuRS with the desired selectivity was isolated. We next attempted a stepwise strategy[15] in which the same selection scheme was used first to evolve an aminoacyl-tRNA synthetase specific for the Anap analogue, 3-(naphthalen-2-ylamino)-2-aminopropanoic acid (Nap, **2**). This amino acid lacks the acyl substituent of Anap and therefore requires a lower degree of hydrogen bonding complementarity in the amino acid binding site of LeuRS. Five rounds of selection generated 92 clones that survived only in the presence of Nap in uracil dropout medium; DNA sequencing of

Table 1. Selected Anap-Specific LeuRS Mutants

LeuRS	frequency	Leu 38	Met 40	Leu 41	Tyr 499	Tyr 500	Tyr 527	His 537	Leu 538	Phe 541	Ala 560
Anap-1	10/10	Phe	Gly	Pro	Gly	Tyr	Ala	Thr	Cys	Ser	Val
Anap-2A	5/10	Phe	Gly	Pro	Val	His	Ala	Glu	Ser	Cys	Val
Aanp-2B	3/10	Phe	Gly	Pro	Ile	His	Ala	Glu	Ser	Cys	Val
Anap-2C	2/10	Phe	Gly	Pro	Val	Leu	Ala	Glu	Ser	Cys	Val

J|A|C|S
PERSPECTIVES

Published on Web 08/18/2009

Synthesis at the Interface of Chemistry and Biology

Xu Wu[‡] and Peter G. Schultz*[,†,‡]

The Scripps Research Institute, 10550 North Torrey Pines Road, La Jolla, California 92037, and Genomics Institute of the Novartis Research Foundation, 10675 John Jay Hopkins Drive, San Diego, California 92121

Received April 1, 2009; E-mail: schultz@scripps.edu

Abstract: As the focus of synthesis increasingly shifts from its historical emphasis on molecular structure to function, improved strategies are clearly required for the generation of molecules with defined physical, chemical, and biological properties. In contrast, living organisms are remarkably adept at producing molecules and molecular assemblies with an impressive array of functions — from enzymes and antibodies to the photosynthetic center. Thus, the marriage of Nature's synthetic strategies, molecules, and biosynthetic machinery with more traditional synthetic approaches might enable the generation of molecules with properties difficult to achieve by chemical strategies alone. Here we illustrate the potential of this approach and overview some opportunities and challenges in the coming years.

Introduction

The feature that perhaps most distinguishes chemistry from the rest of the sciences is the ability of chemists to control the structure of matter at the molecular level — from complex natural products like vancomycin to nanoparticles and whole genomes. Indeed there have been remarkable advances in the fields of total synthesis and synthetic methods over the past 50 years. Unfortunately, we are not nearly as adept at the synthesis of molecules with defined functions as we are at the synthesis of molecules with defined structures. As the focus of chemistry increasingly shifts from structure to function, chemists will need to develop better strategies to efficiently generate molecules, and systems of molecules, with desired physical, chemical, or biological properties in order to meet the biomedical, energy, and environmental needs of the future. Indeed this challenge represents one of the great opportunities for synthesis in the coming years. One direction we can turn for help is Mother Nature — after all, living organisms carry out a remarkable array of complex functions using natural molecules and molecular assemblies, ranging from antibiotics and enzymes to the ribosome and photosynthetic center.

Organic chemists have spent considerable effort synthesizing molecules that attempt to mimic the functions found in Nature. Early examples include functionalized synthetic hosts,[1,2] iron–sulfur clusters,[3] and heme analogues.[4] These efforts attempted to replicate key functions of natural enzymes and receptors and, thereby, give new insight into their molecular mechanisms. As chemists became more sophisticated in their understanding of biomolecules and biological methods, there was an increasing shift in focus to the synthesis of biomolecular mimetics that directly modulate the activities of biological systems themselves. A pioneering example was the synthesis by Dervan and co-workers of polypyrrole-carboxamides that bind DNA in a sequence-specific manner much like transcriptional repressors (Figure 1).[5–7]

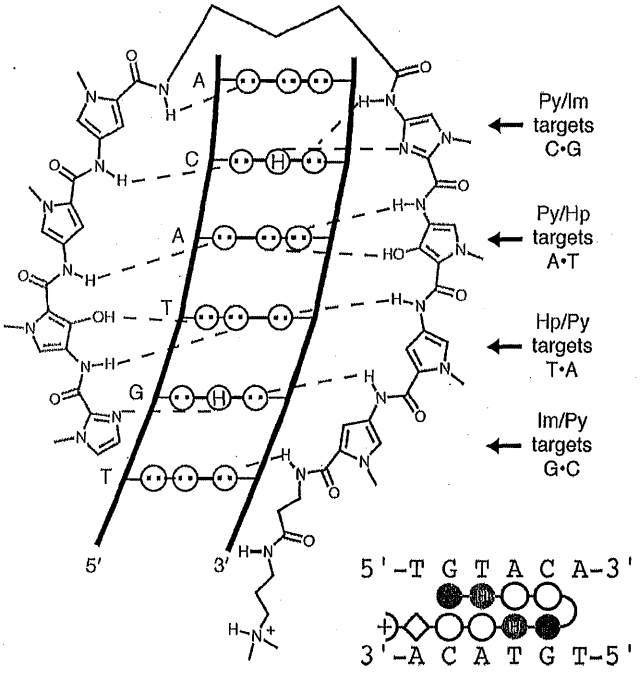

Figure 1. Synthetic molecules that sequence-specifically bind duplex DNA much like transcriptional repressors.[6] Image courtesy of Peter Dervan.

But one need not be limited to chemical synthesis alone to generate molecules with novel functions. One can exploit Nature itself, i.e., use the synthetic strategies, molecules, and biosynthetic machinery of living organisms together with more traditional chemical approaches to generate molecules with properties that might be difficult to realize by either strategy alone. Such an approach represents a marriage of traditional chemical synthesis with the emerging field of synthetic biology.[8] Early efforts in this direction included the generation of semisynthetic enzymes[9] and ion channels[10] by Kaiser and Erlanger, respectively, and the work of Orgel on DNA-directed chemical synthesis.[11] Today this approach is beginning to impact many areas of the chemical, biological, and materials sciences.

[‡] Genomics Institute of the Novartis Research Foundation.
[†] The Scripps Research Institute.

J|A|C|S COMMUNICATIONS

Published on Web 08/13/2009

Photoinduced, Family-Specific, Site-Selective Cleavage of TIM-Barrel Proteins

Nicola Floyd,[†] Neil J. Oldham,[‡] Christopher J. Eyles,[§] Stephen Taylor,[∥] Dmitry A. Filatov,[⊥] Mark Brouard,[§] and Benjamin G. Davis*,[†]

Department of Chemistry, University of Oxford, Chemistry Research Laboratory, Mansfield Road, Oxford, OX1 3TA, U.K., Department of Chemistry, University of Oxford, Physical and Theoretical Chemistry Laboratory, South Parks Road, OX1 3QZ, U.K., The School of Chemistry, University of Nottingham, University Park, Nottingham, NG7 2RD, U.K., Computational Biology Research Group, University of Oxford, Oxford, OX1 3RE, U.K., and Department of Plant Sciences, University of Oxford, South Parks Road, Oxford, OX1 3RB, U.K.

Received April 1, 2009; E-mail: ben.davis@chem.ox.ac.uk

Proteins have long been known to be affected by UV irradiation in processes ranging from amino acid side chain degradation, the reduction of disulfide bridges, aggregation, and even to consequent loss of biological activity.[1−3] However, natural examples of clean, site-selective photocleavage are rare. To the best of our knowledge, the only reported examples are fluorescent proteins Kaede and EosFP that experience cleavage (between Phe61,His62 at 400 nm) and require prior formation of a specific chromophore.[4,5]

A more general, clean, photoinduced cleavage mechanism, with potential biotechnological utility in protein preparation[6] or proteomic analyses,[7,8] is therefore also of fundamental interest. Indeed, while a number of site-selective photolytic methods requiring the addition of extraneous cleavage agents have been investigated,[9−14] these are to date poorly selective and low yielding. Use of unnatural amino acids, such as *o*-nitro-Phe,[15,16] only allows photocleavage in up to ~30%.[17] Unexpectedly, while investigating the photochemical modification of proteins, we have discovered a clean, photocleavage reaction localized to TIM-barrel proteins from family 1 of glycosylhydrolases (GH-1).

UV irradiation of archetypal GH-1 protein from the hyperthermophilic archaeon *Sulfolobus solfataricus* (*Ssβ*G)[18] gave fragment product profiles that were sharp and clean (Scheme 1), suggesting protein cleavage at a single site.[19] To probe reactive transitions precise frequency light (193−355 nm) was generated using (Nd:YAG)-pumped tunable dye and ArF-excimer (193 nm) lasers. No cleavage was observed in the absence of UV light or at wavelengths outside the range ~240−310 nm.

Cleanly formed fragment masses (18.2, 39.1 kDa) were determined by ESI-MS (Scheme 1). *N*-Terminal sequencing revealed the latter to be "blocked" by an unnatural, unreactive residue and the former to share the sequence found at the *N*-terminus of *Ssβ*G, indicating a cleavage site between residues His150 and Trp151. *Ssβ*G mutants containing alterations at this junction (H150A, W151A, H150F) remained intact and did not fragment, giving additional evidence for this specific cleavage site and highlighting the need for specific residues and not simply for potential functional (e.g., aromatic His150→Phe) group equivalents.

Bioinformatic analysis reveals that the His-Trp (HW) diad is widespread and, indeed, is repeated at positions His424Trp425 in *Ssβ*G. Since this site did not dissociate on exposure to UV light, we considered that an extended series of residues bordering His150 and Trp151 must contribute to the remarkable regioselectivity of this cleavage reaction. To probe the underlying molecular contributions, short peptide fragments of *Ssβ*G, expected to have little inherent conformation but correct primary sequence, were synthesized: H-HWP-NH_2 and H-LNMYHWPLPL-NH_2, representing residues 150−152 and 146−155 of *Ssβ*G, respectively. Neither fragmented under UV light.

Scheme 1. Photoinduced Site Selective Cleavage of TIM-Barrel GH-1 Proteins[a]

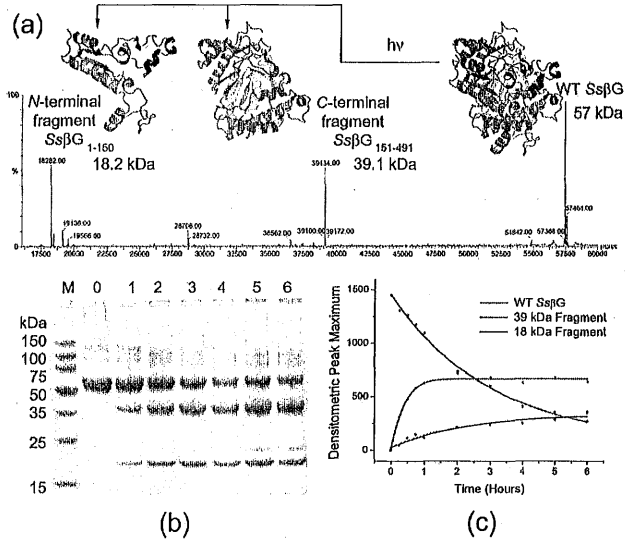

[a] (a) ESI-MS after 1 h irradiation; (b) SDS-PAGE time course analysis 1−6 h; (c) densitometry determined reaction course.

These results implicated conformation and secondary/tertiary structure as key determinants in fragmentation. Ala-scanning was used to probe a 3.5 Å sphere of residues around the cleavage site: *Ssβ*G mutations Y149A, P152A, F222A, and W433A prevented fragmentation, while alteration of more remote residues (Q18A, R79A, N81A, L153A, N205A, E206A, V210A, and E387A) had no effect. Modeling of the cleavage site (Figure 1) reveals that essential residue groups Y149, F222, W433, and P152 cradle residue W151 in an hydrophobic, π-rich environment.

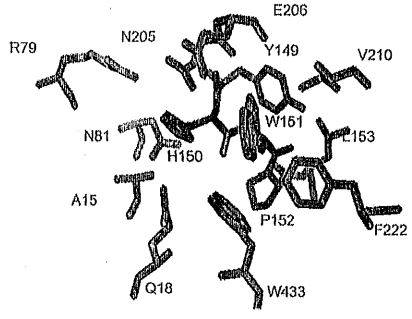

Figure 1. *Ssβ*G's photocleavage site (blue) and associated essential (red) and nonessential (green) residues. Model based on PDB 1gow.

[†] CRL, University of Oxford.
[‡] University of Nottingham.
[§] PTCL, University of Oxford.
[∥] Computational Biology, University of Oxford.
[⊥] Plant Sciences, University of Oxford.

10.1021/ja9026105 CCC: $40.75

JOURNAL OF BACTERIOLOGY, Sept. 2009, p. 5775–5784 Vol. 191, No. 18
0021-9193/09/$08.00+0 doi:10.1128/JB.00521-09

Role of the σ^D-Dependent Autolysins in *Bacillus subtilis* Population Heterogeneity▽†

Rui Chen, Sarah B. Guttenplan, Kris M. Blair, and Daniel B. Kearns*

Department of Biology, Indiana University, 1001 East Third Street, Bloomington, Indiana 47405

Received 17 April 2009/Accepted 16 June 2009

Exponentially growing populations of *Bacillus subtilis* contain two morphologically and functionally distinct cell types: motile individuals and nonmotile multicellular chains. Motility differentiation arises because RNA polymerase and the alternative sigma factor σ^D activate expression of flagellin in a subpopulation of cells. Here we demonstrate that the peptidoglycan-remodeling autolysins under σ^D control, LytC, LytD, and LytF, are expressed in the same subpopulation of cells that complete flagellar synthesis. Morphological heterogeneity is explained by the expression of LytF that is necessary and sufficient for cell separation. Moreover, LytC is required for motility but not at the level of cell separation or flagellum biosynthesis. Rather, LytC appears to be important for flagellar function, and motility was restored to a *LytC* mutant by mutation of either *lonA*, encoding the LonA protease, or a gene encoding a previously unannotated swarming motility inhibitor, SmiA. We conclude that heterogeneous activation of σ^D-dependent gene expression is sufficient to explain both the morphological heterogeneity and functional heterogeneity present in vegetative *B. subtilis* populations.

Growing populations of *Bacillus subtilis* are heterogeneous in cell morphology (17). Some members of these populations grow as single cells that are motile, whereas other cells in the populations grow in multicellular, nonmotile chains. The difference in motility between the two cell types is controlled at the level of gene transcription. The expression of the gene that encodes the flagellar filament (*hag*) is either ON or OFF and is under the control of RNA polymerase and the alternative sigma factor σ^D (9, 17, 29). Cells that are ON for flagellin expression complete flagellum assembly and constitute the motile subpopulation. Cells that are OFF for flagellin expression do not complete flagellum biosynthesis and constitute the nonmotile subpopulation.

The dimorphism of single cells and chaining cells in heterogeneous populations has not been resolved but is likely related to autolysin activity. Autolysins are bacterial enzymes that hydrolyze and remodel the peptidoglycan found in the bacterial cell wall (38, 42). *B. subtilis* is a gram-positive bacterium with a thick layer of peptidoglycan exterior to the cell membrane. During cell division, the cell wall grows inward by a process called septation to divide the mother into two identical daughters. The daughter cells subsequently remain joined by a shared layer of peptidoglycan, and autolysins are required for daughter cell separation (1, 10, 11, 25). Autolysins have also been implicated in cell wall turnover, sporulation, and motility (12, 33, 34, 39).

B. subtilis encodes at least 35 differentially regulated autolysins, but 3 of these autolysins in particular are strong candidates for participating in the single-cell–chain heterogeneity observed during exponential growth: LytC (an *N*-acetylmuramoyl-L-alanine amidase), LytD (an endo-β-*N*-acetylglucosaminidase), and LytF (a γ-D-glutamate *meso*-diaminopimelate muropeptidase) (20, 27, 26, 38). The genes that encode the LytD and LytF autolysins are under exclusive control of σ^D, and 70% of LytC expression is σ^D dependent (15, 20, 21, 26, 27). Furthermore, LytC, LytD, and LytF have been implicated in vegetative cell separation and motility (3, 31, 36). The simultaneous reduction in expression of the three autolysins is thought to account for the observation that a null mutant in which the gene that encodes σ^D is disrupted does not form separate cells and grows constitutively in chains (28).

Here we investigate the contribution of the σ^D-dependent LytC, LytD, and LytF autolysins to population heterogeneity in *B. subtilis*. We determine that the autolysins are expressed in the same subpopulation that expresses the flagellar filament. In an undomesticated strain background (*B. subtilis* 3610) in which the majority of cells in a population are ON for autolysin expression, we find that LytF is dedicated chiefly to cell separation, whereas LytC supports swarming motility. Thus, cells that are ON for σ^D express both the autolysin and flagellar genes and grow as separate motile cells. Cells that are OFF for σ^D do not express the autolysin or flagellar genes and grow as nonmotile chains. Finally, we demonstrate that the requirement of autolysins for motility is related to flagellar function rather than to flagellar biosynthesis or cell separation and that the motility defect could be genetically suppressed.

MATERIALS AND METHODS

Strains and growth conditions. *B. subtilis* strains were grown in Luria-Bertani (LB) broth (10 g tryptone per liter, 5 g yeast extract per liter, 5 g NaCl per liter) or on LB agar plates containing 1.5% Bacto agar at 37°C. When appropriate, antibiotics were included at the following concentrations: 10 μg/ml tetracycline, 100 μg/ml spectinomycin, 5 μg/ml chloramphenicol, 5 μg/ml kanamycin, and 1 μg/ml erythromycin plus 25 μg/ml lincomycin (*mls*). Isopropyl β-D-thiogalactopyranoside (IPTG) (Sigma) was added to the medium at the concentration indicated below when appropriate.

Swarm expansion assay. Cells were grown to mid-log phase at 37°C in LB broth and resuspended at an optical density at 600 nm (OD_{600}) of 10 in 1× PBS (137 mM NaCl, 2.7 mM KCl, 10 mM Na_2HPO_4, 2 mM KH_2PO_4) containing

* Corresponding author. Mailing address: Department of Biology, Indiana University, 1001 East Third Street, Bloomington, IN 47405. Phone: (812) 856-2523. Fax: (812) 856-6705. E-mail: dbkearns@indiana.edu.

† Supplemental material for this article may be found at http://jb.asm.org/.

▽ Published ahead of print on 19 June 2008.

Originally published In Press as doi:10.1074/jbc.M109.026054 on July 1, 2009

J. Biol. Chem., Vol. 284, Issue 36, 23902-23911, September 4, 2009

Generation of Digital Responses in Stress Sensors*[S]

Tània Martiáñez, Sílvia Francès, and José M. López[1]

From the From the Institut de Neurociències i Departament de Bioquímica i Biología Molecular, Unitat de Bioquímica, Facultad de Medicina, Universitat Autònoma de Barcelona, 08193 Cerdanyola del Vallès, Barcelona, Spain

This Article
- Full Text
- Full Text (PDF)
- Supplemental Data
- All Versions of this Article: 284/36/23902 *most recent* M109.026054v1
- Submit a Letter to Editor
- Alert me when this article is cited
- Alert me when eLetters are posted
- Alert me if a correction is posted
- Citation Map

Services
- Email this article to a friend
- Similar articles in this journal
- Similar articles in PubMed
- Alert me to new issues of the journal
- Download to citation manager
- Request Permissions

Google Scholar
- Articles by Martiáñez, T.
- Articles by López, J. M.

PubMed
- PubMed Citation
- Articles by Martiáñez, T.
- Articles by López, J. M.

Social Bookmarking
What's this?

ABSTRACT

Ultrasensitivity, hysteresis (a form of biochemical memory), and all-or-none (digital) responses are important signaling properties for the control of irreversible processes and are well characterized in the c-Jun N-terminal kinase (JNK) system using *Xenopus* oocytes. Our aim was to study these properties in the AMP-activated protein kinase (AMPK) signaling system under stress conditions that could engage a cell death program, and compare them to the JNK responses. After characterization of *Xenopus* AMPK, we show here that the response to antimycin (nonapoptotic) was slightly cooperative and graded (analog) in individual oocytes, whereas the response to sorbitol (which induced cytochrome *c* release and caspase activation) was ultrasensitive, digital in single cells, and without hysteresis, hallmarks of a monostable system. Moreover, initial graded responses of AMPK and JNK turned into digital during a critical period for the execution of the cell death program, although single cell analysis did not show complete correlation between AMPK or JNK activation and cytochrome *c* release. We propose a model where the life or death decision in the cell is made by integration of multiple digital signals from stress sensors.

Received for publication, May 27, 2009

[1] Recipient of a contract from the "Programa Ramón y Cajal" (MEC). To whom correspondence should be addressed: Institut de Neurociències, Edifici M, Campus de Bellaterra, Universitat Autònoma de Barcelona, 08193 Cerdanyola del Vallès, Barcelona, Spain. Tel.: 34-93-5814278; Fax: 34-93-5811573; E-mail: josemanuel.lopez@uab.es.

CiteULike Complore Connotea Del.icio.us Digg Reddit Technorati What's this?

Originally published In Press as doi:10.1074/jbc.M109.011973 on July 14, 2009

J. Biol. Chem., Vol. 284, Issue 37, 24981-24987, September 11, 2009

Defective Chromatin Structure in Somatic Cell Cloned Mouse Embryos*[S]

Miao Zhang[‡§1], **Fengchao Wang**[§1], **Zhaohui Kou**[§], **Yu Zhang**[§], **and Shaorong Gao**[§2]

From the From the [‡]College of Biological Sciences, China Agricultural University, Beijing 100094, China and , the [§]National Institute of Biological Sciences, Beijing 102206, China

This Article

- Full Text
- Full Text (PDF)
- Supplemental Data
- All Versions of this Article: 284/37/24981 *most recent* M109.011973v1
- Submit a Letter to Editor
- Alert me when this article is cited
- Alert me when eLetters are posted
- Alert me if a correction is posted
- Citation Map

Services

- Email this article to a friend
- Similar articles in this journal
- Similar articles in PubMed
- Alert me to new issues of the journal
- Download to citation manager
- Request Permissions

Google Scholar

- Articles by Zhang, M.
- Articles by Gao, S.

PubMed

- PubMed Citation
- Articles by Zhang, M.
- Articles by Gao, S.

Social Bookmarking

What's this?

ABSTRACT

Epigenetic reprogramming plays a central role in the development of cloned embryos generated by somatic cell nuclear transfer, and it is believed that aberrant reprogramming leads to the abnormal development of most cloned embryos. Recent studies show that trimethylation of H3K27 (H3K27me3) contributes to the maintenance of embryonic stem cell pluripotency because the differentiation genes are always occupied by nucleosomes trimethylated at H3K27, which represses gene expression. Here, we provide evidence that differential H3K27me3 modification exists between normal fertilization-produced blastocysts and somatic cell nuclear transfer cloned blastocysts; H3K27me3 was specifically found in cells of the inner cell mass (ICM) of normal blastocysts, whereas there was no modification of H3K27me3 in the ICM of cloned blastocysts. Subsequently, we demonstrated that the differentiation-related genes, which are marked by H3K27me3 in embryonic stem cells, were expressed at significantly higher levels in cloned embryos than in normal embryos. The polycomb repressive complex 2 (PRC2) component genes (Eed, Ezh2, and Suz12), which are responsible for the generation of H3K27me3, were expressed at lower levels in the cloned embryos. Our results suggest that reduced expression of PRC2 component genes in cloned embryos results in defective modification of H3K27me3 to the differentiation-related genes in pluripotent ICM cells. This results in premature expression of developmental genes and death of somatic cloned embryos shortly after implantation. Taken together, these studies suggest that H3K27me3 might be an important epigenetic marker with which to evaluate the developmental potential of cloned embryos.

Received for publication, April 22, 2009 , and in revised form, July 10, 2009.

FOOTNOTES

[1] Both authors contributed equally to this work.

[2] To whom correspondence should be addressed: National Institute of Biological Sciences, Beijing 102206, China.

Originally published In Press as doi:10.1074/jbc.M109.007948 on July 14, 2009

J. Biol. Chem., Vol. 284, Issue 37, 25015-25025, September 11, 2009

Gene Looping Is Conferred by Activator-dependent Interaction of Transcription Initiation and Termination Machineries*[S]

Belal El Kaderi, Scott Medler, Sarita Raghunayakula, and Athar Ansari[1]

From the From the Department of Biological Science, Wayne State University, Detroit, Michigan 48202

ABSTRACT

Gene looping juxtaposes the promoter and terminator regions of RNA polymerase II-transcribed genes in yeast and mammalian cells. Here we report an activator-dependent interaction of transcription initiation and termination factors during gene looping in budding yeast. Chromatin analysis revealed that *MET16*, *INO1*, and *GAL1p-BUD3* are in a stable looped configuration during activated transcription. Looping was nearly abolished in the absence of transcription activators Met28, Ino2, and Gal4 of *MET16*, *INO1*, and *GAL1p-BUD3* genes, respectively. The activator-independent increase in transcription was not accompanied by loop formation, thereby suggesting an essential role for activators in gene looping. The activators did not facilitate loop formation directly because they did not exhibit an interaction with the 3' end of the genes. Instead, activators physically interacted with the general transcription factor TFIIB when the genes were activated and in a looped configuration. TFIIB cross-linked to both the promoter and the terminator regions during the transcriptionally activated state of a gene. The presence of TFIIB on the terminator was dependent on the Rna15 component of CF1 3' end processing complex. Coimmunoprecipitation revealed a physical interaction of Rna15 with TFIIB. We propose that the activators facilitate gene looping through their interaction with TFIIB during transcriptional activation of genes.

This Article
- Full Text
- Full Text (PDF)
- Supplemental Data
- All Versions of this Article: 284/37/25015 *most recent* M109.007948v1
- Submit a Letter to Editor
- Alert me when this article is cited
- Alert me when eLetters are posted
- Alert me if a correction is posted
- Citation Map

Services
- Email this article to a friend
- Similar articles in this journal
- Similar articles in PubMed
- Alert me to new issues of the journal
- Download to citation manager
- Request Permissions

Google Scholar
- Articles by El Kaderi, B.
- Articles by Ansari, A.

PubMed
- PubMed Citation
- Articles by El Kaderi, B.
- Articles by Ansari, A.

Social Bookmarking
What's this?

Received for publication, April 14, 2009 , and in revised form, June 18, 2009.

[1] To whom correspondence should be addressed: Dept. of Biological Science, Wayne State University, 5047 Gullen Mall, Detroit, MI 48202. Tel.: 313-577-9251; Fax: 313-571-6891; E-mail: bb2749@wayne.edu.

CiteULike Complore Connotea Del.icio.us Digg Reddit Technorati What's this?

Published August 17, 2009

Myosin-driven peroxisome partitioning in *S. cerevisiae*

Andrei Fagarasanu,[1] Fred D. Mast,[1] Barbara Knoblach,[1] Yui Jin,[3] Matthew J. Brunner,[3] Michael R. Logan,[1] J.N. Mark Glover,[2] Gary A. Eitzen,[1] John D. Aitchison,[4] Lois S. Weisman,[3] and Richard A. Rachubinski[1]

[1]Department of Cell Biology and [2]Department of Biochemistry, University of Alberta, Edmonton, Alberta T6G 2H7, Canada
[3]Life Sciences Institute, Department of Cell and Developmental Biology, University of Michigan, Ann Arbor, MI 48109
[4]Institute for Systems Biology, Seattle, WA 98103

In *Saccharomyces cerevisiae*, the class V myosin motor Myo2p propels the movement of most organelles. We recently identified Inp2p as the peroxisome-specific receptor for Myo2p. In this study, we delineate the region of Myo2p devoted to binding peroxisomes. Using mutants of Myo2p specifically impaired in peroxisome binding, we dissect cell cycle–dependent and peroxisome partitioning–dependent mechanisms of Inp2p regulation. We find that although total Inp2p levels oscillate with the cell cycle, Inp2p levels on individual peroxisomes are controlled by peroxisome inheritance, as Inp2p aberrantly accumulates and decorates all peroxisomes in mother cells when peroxisome partitioning is abolished. We also find that Inp2p is a phosphoprotein whose level of phosphorylation is coupled to the cell cycle irrespective of peroxisome positioning in the cell. Our findings demonstrate that both organelle positioning and cell cycle progression control the levels of organelle-specific receptors for molecular motors to ultimately achieve an equidistribution of compartments between mother and daughter cells.

Introduction

Membrane-bound organelles organize the eukaryotic cell into distinct compartments that are each specialized for specific cellular functions. Compartmentalization allows a range of different processes to occur simultaneously within optimal microenvironments to increase the overall metabolic efficiency of cells. To maintain the advantages of compartmentalization, eukaryotic cells have evolved molecular mechanisms to ensure the faithful inheritance of their organelles during cell division.

The yeast *Saccharomyces cerevisiae* divides asymmetrically by budding. The accurate inheritance of its organelles is achieved by delivery of a portion of its organelles to the bud concomitant with retention of the remaining organelles in the mother cell (Fagarasanu and Rachubinski, 2007). This feature makes detection and isolation of mutants defective in organelle partitioning easier in budding yeast than in cells that divide by median fission, thus facilitating investigation of the spatial and temporal control of organelle motility.

The bud-directed movement of organelles is mediated by class V myosins, which are motors specialized in carrying cargo along actin filaments. The amino termini of all class V myosins contain a conserved motor domain that generates actin-based movements, whereas their divergent carboxyl termini form a globular domain called the tail that is specialized in capturing various organelles. Myo2p and Myo4p are the *S. cerevisiae* class V myosins (for reviews see Reck-Peterson et al., 2000; Bretscher, 2003; Pruyne et al., 2004). Myo4p is involved in the movement of cortical ER (Estrada et al., 2003), whereas Myo2p powers the bud-directed movement of most other membrane-bound organelles, including Golgi elements (Rossanese et al., 2001), the vacuole (Ishikawa et al., 2003; Tang et al., 2003), peroxisomes (Hoepfner et al., 2001; Fagarasanu et al., 2006a), and mitochondria (Itoh et al., 2002, 2004; Boldogh et al., 2004; Altmann et al., 2008). Myo2p also drives the polarized transport of secretory vesicles, which is essential for cell growth (Govindan et al., 1995; Schott et al., 1999), and carries the plus ends of cytoplasmic microtubules into the bud for orientation of the nucleus before mitosis (Yin et al., 2000).

Ensuring the efficient transport of the different types of organelles carried by Myo2p requires tight control and coordination of Myo2p's attachment to and detachment from different

Correspondence to Richard A. Rachubinski: rick.rachubinski@ualberta.ca

Abbreviations used in this paper: CSM, complete supplement mixture; G6PDH, glucose-6-phosphate dehydrogenase; MBP, maltose-binding protein; mRFP, monomeric RFP; pA, protein A.

The Rockefeller University Press $30.00
J. Cell Biol. Vol. 186 No. 4 541–554
www.jcb.org/cgi/doi/10.1083/jcb.200904050

Efficient exact and *K*-skip methods for stochastic simulation of coupled chemical reactions

Xiaodong Cai[a] and Ji Wen
Department of Electrical and Computer Engineering, University of Miami, Coral Gables, Florida 33124, USA

(Received 27 February 2009; accepted 22 July 2009; published online 12 August 2009)

Gillespie's direct method (DM) [D. Gillespie, J. Chem. Phys. **81**, 2340 (1977)] for exact stochastic simulation of chemical reaction systems has been widely adopted. It is easy to implement but requires large computation for relatively large systems. Recently, two more efficient methods, next reaction method (NRM) [M. A. Gibson and J. Bruck, J. Phys. Chem. A **105**, 1876 (2000)] and optimized DM (ODM) [Y. Cao *et al.*, J. Chem. Phys. **121**, 4059 (2004)], have been developed to improve simulation speed. It has been demonstrated that the ODM is the state-of-the-art most efficient method for exact stochastic simulation of most practical reaction systems. In this paper, we first develop an exact stochastic simulation algorithm named ODMK that is more efficient than the ODM. We then develop an approximate method named *K*-skip method to further accelerate simulation. Using two chemical reaction systems, we demonstrate that our ODMK and *K*-skip method can save 20%–30% and 70%–80% simulation time, respectively, comparing to the ODM. We also show that our ODMK and *K*-skip method provide almost the same simulation accuracy as the ODM. © *2009 American Institute of Physics*. [DOI: 10.1063/1.3204422]

I. INTRODUCTION

In certain chemical reaction systems such as cells in living organisms, the dynamics of the system are often dominated by the action of a small number of molecules, and thus exhibit significant stochastic fluctuations. Such random fluctuations in the number of molecules appear to have many important consequences in biology.[1–3] For example, the stochasticity in gene expression can generate phenotypic heterogeneity in a bacterial population of isogenic cells.[1] Therefore, in computational modeling and simulation of chemical reaction systems, it is important to have an appropriate method to reflect the stochasticity in system dynamics. Gillespie developed a stochastic simulation algorithm (SSA) to simulate every reaction event in a chemical reaction system, when the time evolves.[4,5] Gillespie's SSA is exact in the sense that it is developed rigorously based upon the microphysical premise of stochastic chemical kinetics for well-stirred chemical reaction systems.[5,6]

Although Gillespie's exact SSA is easy to implement and produces system dynamics with correct statistics, it requires large computation especially for systems where the number of reaction channels and/or the number of molecules are large. A more efficient exact stochastic simulation method, named next reaction method (NRM), was developed by Gibson and Bruck.[7] In the next reaction method, two sophisticated data structures are employed to save computation, thereby improving simulation speed. An optimized direct method (ODM) for exact stochastic simulation was proposed by Cao *et al.*[8] It was demonstrated that the ODM is much faster than Gillespie's direct method (DM) and, in general, faster than the NRM in simulating practical reaction systems. Several approximate leap methods, including τ-leap,[9,10] binomial τ-leap,[11,12] multinomial τ-leap,[13] unbiased τ-leap,[14] and *K*-leap methods,[15,16] were also developed to accelerate stochastic simulation at the price of reduced simulation accuracy.

In this paper, we develop an exact SSA, named ODMK, which is more efficient than the ODM. In the DM and the ODM, two random variables are generated to simulate the occurrence of each reaction, one for the reaction index and the other for the random time between the occurrences of two consecutive reactions. In our ODMK, we use only one random variable to generate a sequence of $K>1$ reaction indices. Since the number of random variables generated is reduced, our exact SSA is faster than existing exact SSAs. We further develop an approximate method, named *K*-skip method, where we generate the random time between the occurrence of every $K>1$ reactions, skipping generation of the random time between the occurrence of two consecutive reactions. Since the random variables generated in our *K*-skip method is two per *K* reactions, which is much smaller than two per reaction in the DM and the ODM, our *K*-skip can significantly improve simulation speed especially when *K* is large. Our numerical results demonstrate that our *K*-skip method yields almost the same accuracy as the exact SSA.

The rest of this paper is organized as follows. In Sec. II, we describe the chemical reaction system under consideration and briefly review current exact SSAs. In Sec. III, we develop our ODMK. In Sec. IV, we derive our *K*-skip method. In Sec. V, we present two numerical examples to illustrate our algorithms, and compare their performance with that of the ODM. Finally, conclusions are drawn in Sec. VI.

[a]Author to whom correspondence should be addressed. Electronic mail: x.cai@miami.edu. Tel./Fax: (305) 284-5329/4044.

Lab on a Chip RSC Publishing

Journals Lab on a Chip Contents List DOI: 10.1039/b903608c

Lab Chip, 2009, 9, 2665-2672 | DOI: 10.1039/b903608c | Paper

A fast and efficient microfluidic system for highly selective one-to-one droplet fusion†‡

Linas Mazutis , Jean-Christophe Baret and Andrew D. Griffiths *

Institut de Science et d'Ingénierie Supramoléculaires (ISIS), Université de Strasbourg, 67083, Strasbourg Cedex, France. E-mail: griffiths@unistra.fr; Fax: +33 90245115

Received 23rd February 2009 , Accepted 21st May 2009

First published on the web 12th June 2009

Microdroplets in microfluidic systems can be used as independent microreactors to perform a range of chemical and biological reactions. However, in order to add new reagents to pre-formed droplets at defined times, to start, modify, or terminate a reaction, it is necessary to perform a controlled fusion with a second droplet. We describe and characterize a simple and extremely reliable technique for the one-to-one fusion of droplet pairs in a microfluidic system at kHz frequencies. The technique does not require special channel treatment, electrical fields or lasers to induce droplet fusion. Instead, we make use of transient states in the stabilization of the droplet interface by surfactant, coupled to a proper geometrical design of a coalescence module, to induce the selective fusion of a droplet stabilized by surfactant (re-injected) with a droplet which is not fully stabilized (generated on-chip). Using a 1.2-fold excess of the surfactant-stabilized droplets ~99% of the partially stabilized droplets were fused one-to-one with surfactant-stabilized droplets. Even when the surfactant-stablized droplets were in 5-fold excess, over 96% of the partially stabilized droplets were fused one-to-one. The fused droplet contains enough surfactant to inhibit further fusion events. After fusion, the droplets were fully stabilized by additional surfactant provided in the carrier oil, which allowed the fused droplets to be collected, incubated off-chip and re-injected onto a microfluidic device without any undesired coalescence.

1. Introduction

All but the simplest reactions and assays require multiple steps where new reagents are added between steps. In microtitre-plate based systems this is achieved by pipetting in new reagents at defined times. However, even using sophisticated (and expensive) robotic liquid-handling systems the throughput is little more than one per second. The quest for higher throughput is, of necessity, driving the development of ever smaller reaction vessels. However, there is little scope to further reduce reaction volumes below the current minimum of 1–2 μL using microtitre plate technology.

One option is to use microdroplets in water-in-oil emulsions as microreactors: the droplets have volumes 10^3 to 10^9 times smaller than the smallest working volume in a microtitre plate well. *In Vitro* Compartmentalization (IVC)[1] of reactions in emulsions was initially developed for directed evolution and has allowed the selection of a wide range of proteins and RNAs for binding, catalytic and regulatory activities.[2] Other applications rapidly followed, notably massively parallel PCR of single DNA molecules (emulsion PCR), which is used, for example, for two commercial 'next-generation' high-throughput sequencing systems.[3]

However, it is difficult to add reagents to droplets in bulk emulsions after they are formed,[2] which is a serious limitation. This problem can potentially be overcome by using microfluidic systems, in which controlled droplet fusion is possible. Pairs of large (usually >100 nL) droplets can be fused using electrowetting in digital microfluidic systems,[4] but the number of discrete fluidic operations per second is relatively low (<0.1 kHz).[5] Alternatively, high numbers of droplets (>10^7), with volumes as small as 1 pL, flowing in a carrier oil, can be fused in pairwise fashion at high frequencies (>kHz) in droplet-based microfluidic systems. There are several ways to fuse aqueous droplets using droplet-based microfluidic systems. Droplets that are not stabilized by surfactant will coalesce spontaneously,[6–11] or can be coalesced based on a surface energy pattern on the walls of a microfluidic device,[12,13] or a new stream of fluid can be merged with large droplets passing an orifice.[14,15] Surfactant stabilized droplets can be fused using local heating from a focused laser[16] or using electric forces[17,18] and electro-coalescence has been used to measure millisecond enzyme kinetics[19] and for the synthesis of magnetic iron oxide nanoparticles.[20]

The main problem in droplet coalescence for biological or chemical applications is the existance of two contradictory

Molecular Microbiology (2009) 73(5), 737–741 ■

doi:10.1111/j.1365-2958.2009.06806.x
First published online 29 July 2009

MicroCommentary

An RNA trap helps bacteria get the most out of chitosugars

Jörg Vogel*
Max Planck Institute for Infection Biology, RNA Biology Group, Charitéplatz 1, 10117 Berlin, Germany.

Summary

Small regulatory RNAs (sRNAs) are well known to command bacterial protein synthesis by modulating the translation and decay of target mRNAs. Most sRNAs are specifically regulated by a cognate transcription factor under certain growth or stress conditions. Investigations of the conserved Hfq-dependent MicM sRNA in *Escherichia coli* (article by Poul Valentin-Hansen and colleagues in this issue of *Molecular Microbiology*) and in *Salmonella* have unravelled a novel type of gene regulation in which the chitobiose operon mRNA acts as an RNA trap to degrade the constitutively expressed MicM sRNA, thereby alleviating MicM-mediated repression of the synthesis of the YbfM porin that is required for chitosugar uptake. The results suggest that 'target' mRNAs might be both prey and also predators of sRNAs.

Bacteria are known to produce large numbers of small RNAs (sRNAs), many of which act as post-transcriptional regulators by base-pairing to mRNAs (Waters and Storz, 2009). Since the serendipitous discovery of MicF sRNA as a post-transcriptional repressor of OmpF porin synthesis, the functional characterization of *Escherichia coli* and *Salmonella* sRNAs has shown that almost a third of them repress the synthesis of porins and other outer membrane proteins (Guillier *et al.*, 2006; Vogel and Papenfort, 2006). The ~84 nucleotide MicM sRNA is the latest arrival in the field of enterobacterial porin regulators. The *micM* gene (also known as *sroB* or *rybC*) was discovered in the *ybaK-ybaP* intergenic region (IGR) in genome-wide screens for new sRNAs in *E. coli* (Vogel *et al.*, 2003; Zhang *et al.*, 2003). In both *E. coli* and *Salmonella*, MicM was also observed to be tightly associated with the bacterial sRNA chaperone, Hfq (Zhang *et al.*, 2003; Sittka *et al.*, 2008), indicating that it acts on *trans*-encoded target mRNAs by short antisense pairing (Waters and Storz, 2009).

In an earlier issue of *Molecular Microbiology* this year, Poul Valentin-Hansen and colleagues identified the *ybfM* mRNA encoding a porin of, at the time, unknown specificity as a major target of MicM (Rasmussen *et al.*, 2009). Like many other porin regulators (Guillier *et al.*, 2006; Vogel and Papenfort, 2006), MicM repressed *ybfM* mRNA by Hfq-dependent pairing with the ribosome binding site (RBS) (Rasmussen *et al.*, 2009), inhibiting translational initiation and, thereby, destabilizing this messenger (Fig. 1A, left part). On the face of it, MicM/*ybfM* seemed to be quite an ordinary case of post-transcriptional porin repression.

In this issue of *Molecular Microbiology*, the Valentin-Hansen laboratory reports an exciting turn in the MicM story. They have discovered an RNA trapping mechanism in which MicM itself becomes the target of a functionally related mRNA in order to derepress the *ybfM* target mRNA (Overgaard *et al.*, 2009). The study was motivated by several intriguing and unique observations. Unlike many stress-responsive sRNA genes, the *micM* gene is almost constitutively expressed (Vogel *et al.*, 2003) and does not show evidence for a conserved transcription factor binding site in its promoter region (Mandin and Gottesman, 2009; Rasmussen *et al.*, 2009). The abundant MicM sRNA seemed to be in permanent excess over its target, because the *ybfM* mRNA was hardly detectable under standard growth conditions (Sittka *et al.*, 2008; Overgaard *et al.*, 2009; Rasmussen *et al.*, 2009). In addition, a seminal paper by the Gottesman lab (Massé *et al.*, 2003) had shown that several Hfq-associated sRNAs using the same RBS pairing mechanism as MicM were degraded along with their target mRNAs by the major endoribonuclease, RNase E, suggesting that sRNAs act stoichiometrically. However, overexpression of *ybfM* RNA did not destabilize MicM, arguing against a coupled degradation in this case. Collectively, how would the repression ever be overcome to permit YbfM synthesis?

A genetic screen for factors that could prevent MicM from repressing *ybfM* provided the surprising answer. Aside from two enzymes with established functions in RNA metabolism, poly(A) polymerase (Kushner, 2004)

Accepted 14 July, 2009. *For correspondence. E-mail vogel@mpiib-berlin.mpg.de; Tel. (+49) 30 28460 265; Fax (+49) 30 28460 244.

Molecular Systems Biology 5; Article number 300; doi:10.1038/msb.2009.61
Citation: *Molecular Systems Biology* 5:300

www.molecularsystemsbiology.com

molecular systems biology

REPORT

Control and signal processing by transcriptional interference

Antoine Buetti-Dinh[1], Rosemarie Ungricht[1], János Z Kelemen, Chetak Shetty, Prasuna Ratna and Attila Becskei*

Institute of Molecular Biology, University of Zurich, Zurich, Switzerland
[1] These authors contributed equally to this work
* Corresponding author. Institute of Molecular Biology, University of Zurich, Winterthurerstrasse 190, Zurich 8057, Switzerland.
Tel.: +41 44 635 3180; Fax: +41 44 635 6811; E-mail: attila.becskei@molbio.uzh.ch

Received 28.11.08; accepted 21.7.09

A transcriptional activator can suppress gene expression by interfering with transcription initiated by another activator. Transcriptional interference has been increasingly recognized as a regulatory mechanism of gene expression. The signals received by the two antagonistically acting activators are combined by the polymerase trafficking along the DNA. We have designed a dual-control genetic system in yeast to explore this antagonism systematically. Antagonism by an upstream activator bears the hallmarks of competitive inhibition, whereas a downstream activator inhibits gene expression non-competitively. When gene expression is induced weakly, the antagonistic activator can have a positive effect and can even trigger paradoxical activation. Equilibrium and non-equilibrium models of transcription shed light on the mechanism by which interference converts signals, and reveals that self-antagonism of activators imitates the behavior of feed-forward loops. Indeed, a synthetic circuit generates a bell-shaped response, so that the induction of expression is limited to a narrow range of the input signal. The identification of conserved regulatory principles of interference will help to predict the transcriptional response of genes in their genomic context.
Molecular Systems Biology **5:** 300; published online 18 August 2009; doi:10.1038/msb.2009.61
Subject Categories: synthetic biology; chromatin & transcription
Keywords: noncoding transcription; promoter; repression

Introduction

One of the major goals of quantitative modeling of gene regulation is to predict gene expression based on the occupancy of gene regulatory sites by transcriptional factors. The action of transcriptional activators and repressors bound to a promoter can be represented as a mathematical operation. These operations have been systematically analyzed in prokaryotes (Buchler *et al*, 2003; Hermsen *et al*, 2006; Cox *et al*, 2007), and in eukaryotes (Ratna *et al*, 2009).

The above models focused on the classical role of transcriptional activators: the enhancement of gene expression. Interestingly, activators can also suppress gene expression by, at least, two different mechanisms (Shearwin *et al*, 2005).

First, intergenic transcription initiated by activators from upstream sequences can interfere with the expression of downstream genes. This upstream interference has been observed for the *SER3*, *ADH1* and *ADH3* genes in yeast (Martens *et al*, 2004, 2005; Bird *et al*, 2006). Intergenic transcription produces noncoding RNAs that have been detected in *Saccharomyces cerevisiae* and higher eukaryotes in large numbers (Hongay *et al*, 2006; Khaitovich *et al*, 2006; Neil *et al*, 2009; Xu *et al*, 2009). Positive regulatory aspects of transcriptional interference have been increasingly recognized in processes and phenomena, such as T-cell receptor recombination, latency of the HIV infection and epigenetic cellular memory (Schmitt *et al*, 2005; Abarrategui and Krangel, 2007; Lenasi *et al*, 2008).

Second, when an activator binds to a site that overlaps or is positioned downstream of the transcriptional initiation site, it can interfere with transcriptional initiation and elongation. This downstream antagonism is exemplified by the *ZRT2*, *PRY3* and *ACC1* genes (Li and Johnston, 2001; Bird *et al*, 2004; Bickel and Morris, 2006).

Signals passed onto transcriptional activators that either interfere with transcriptional initiation or initiate intergenic

Molecular Systems Biology 5; Article number 299; doi:10.1038/msb.2009.58
Citation: *Molecular Systems Biology* 5:299

www.molecularsystemsbiology.com

molecular systems biology

Positive selection for elevated gene expression noise in yeast

Zhihua Zhang, Wenfeng Qian and Jianzhi Zhang*

Department of Ecology and Evolutionary Biology, University of Michigan, Ann Arbor, MI, USA
* Correspondence: Department of Ecology and Evolutionary Biology, University of Michigan, 1075 Natural Science Building, 830 North University Avenue, Ann Arbor, MI 48109, USA. Tel.: +1 734 763 0527; Fax: +1 734 763 0544; E-mail: jianzhi@umich.edu

Received 18.11.08; accepted 9.7.09

It is well known that the expression noise is lessened by natural selection for genes that are important for cell growth or are sensitive to dosage. In theory, expression noise can also be elevated by natural selection when noisy gene expression is advantageous. Here we analyze yeast genome-wide gene expression noise data and show that plasma-membrane transporters show significantly elevated expression noise after controlling all confounding factors. We propose a model that explains why and under what conditions elevated expression noise may be beneficial and subject to positive selection. Our model predicts and the simulation confirms that, under certain conditions, expression noise also increases the evolvability of gene expression by promoting the fixation of favorable expression level-altering mutations. Indeed, yeast genes with higher noise show greater between-strain and between-species divergences in expression, even when all confounding factors are excluded. Together, our theoretical model and empirical results suggest that, for yeast genes such as plasma-membrane transporters, elevated expression noise is advantageous, is subject to positive selection, and is a facilitator of adaptive gene expression evolution.
Molecular Systems Biology **5:** 299; published online 18 August 2009; doi:10.1038/msb.2009.58
Subject Categories: functional genomics; simulation and data analysis
Keywords: adaptive evolution; expression noise; plasma-membrane transporters; positive selection; yeast

Introduction

Gene expression, as other biological processes, is subject to noise (Schrodinger, 1944), which is defined as the stochastic variation in the expression level of a gene among isogenic cells under the same condition. Here and elsewhere in the paper, expression level refers to the level of the protein product of the gene, as expression noise is usually measured at the level of protein. Gene expression noise has been measured in prokaryotes (Elowitz *et al*, 2002; Ozbudak *et al*, 2002; Rosenfeld *et al*, 2005), unicellular eukaryotes (Blake *et al*, 2003; Raser and O'Shea, 2004), and mammalian cells (Ramsey *et al*, 2006). These and other studies showed that the level of expression noise varies substantially among genes, is determined genetically, and is selectable (Blake *et al*, 2006; Newman *et al*, 2006; Maheshri and O'Shea, 2007; Ansel *et al*, 2008). Expression noise has both intrinsic and extrinsic sources (Orphanides and Reinberg, 2002; Rao *et al*, 2002; Blake *et al*, 2003; Kaern *et al*, 2005; Raser and O'Shea, 2004, 2005; Bar-Even *et al*, 2006; Newman *et al*, 2006; Volfson *et al*, 2006). Stochastic events in gene expression, including those in transcription initiation, mRNA degradation, translation initiation, and protein degradation, generate intrinsic noise (Raser and O'Shea, 2005). Differences between cells, either in local environment or in the concentration or activity of any factor influencing gene expression, generate extrinsic noise (Raser and O'Shea, 2005). We focus on intrinsic noise in this study because only intrinsic noise is an intrinsic property of a gene.

Gene expression noise is often considered a two-edged sword. On one hand, the noise could be deleterious because it ruins cellular homeostasis in metabolism and developmental programs, affects precise controls of biochemical processes in cells, and breaks the stoichiometric balances among members of protein complexes (Fraser *et al*, 2004; Batada *et al*, 2006; Lehner, 2008). Increased gene expression noise has been reported to result in disease (Cook *et al*, 1998; Kemkemer *et al*, 2002; Bahar *et al*, 2006). Several studies showed direct and indirect evidence for lessened expression noise of genes that are important to cell growth or sensitive to dosage (Fraser *et al*, 2004; Newman *et al*, 2006; Batada and Hurst, 2007; Lehner, 2008). Furthermore, various molecular mechanisms and regulatory network structures (e.g. negative feedbacks) are found to attenuate expression noise (Becskei and Serrano, 2000; Pedraza and van Oudenaarden, 2005). On the other

LETTERS

Adult mice generated from induced pluripotent stem cells

Michael J. Boland[1]*, Jennifer L. Hazen[1]*, Kristopher L. Nazor[1]*, Alberto R. Rodriguez[2], Wesley Gifford[3], Greg Martin[2], Sergey Kupriyanov[2] & Kristin K. Baldwin[1]

Recent landmark experiments have shown that transient overexpression of a small number of transcription factors can reprogram differentiated cells into induced pluripotent stem (iPS) cells that resemble embryonic stem (ES) cells[1–7]. These iPS cells hold great promise for medicine because they have the potential to generate patient-specific cell types for cell replacement therapy and produce *in vitro* models of disease, without requiring embryonic tissues or oocytes[8–10]. Although current iPS cell lines resemble ES cells, they have not passed the most stringent test of pluripotency by generating full-term or adult mice in tetraploid complementation assays[3,11], raising questions as to whether they are sufficiently potent to generate all of the cell types in an organism. Whether this difference between iPS and ES cells reflects intrinsic limitations of direct reprogramming is not known. Here we report fertile adult mice derived entirely from iPS cells that we generated by inducible genetic reprogramming of mouse embryonic fibroblasts. Producing adult mice derived entirely from a reprogrammed fibroblast shows that all features of a differentiated cell can be restored to an embryonic level of pluripotency without exposure to unknown ooplasmic factors. Comparing these fully pluripotent iPS cell lines to less developmentally potent lines may reveal molecular markers of different pluripotent states. Furthermore, mice derived entirely from iPS cells will provide a new resource to assess the functional and genomic stability of cells and tissues derived from iPS cells, which is important to validate their utility in cell replacement therapy and research applications.

Historically, the only way to generate an adult mammal was by fertilization. Advances in somatic cell nuclear transfer (SCNT) have now produced genetically identical mouse clones from a variety of differentiated cell types, from fibroblasts to neurons[12,13]. Similarly, genetically identical adult mice may be derived from ES (or SCNT-ES) cells by tetraploid blastocyst complementation, in which all adult tissues derive from the stem cell line whereas extraembryonic tissues are supplied by the tetraploid cells[14,15]. For unknown reasons, current iPS cell lines have not generated adult or full-term mice in tetraploid complementation assays. This finding, and recent reports of reproducible gene expression differences between iPS and ES cells, suggests that direct reprogramming may be insufficient to restore differentiated cells to full pluripotency, as measured by ES cell equivalence[3,11,16]. Autonomous generation of mice from iPS cells would validate direct reprogramming as equivalent to reprogramming by SCNT, establish iPS cells as functional substitutes for ES cells, and provide a new method to generate adult mice from differentiated cells.

To conclusively demonstrate that iPS cell lines can generate adult mice in tetraploid complementation assays, we designed a genetic marking strategy to distinguish between host blastocyst and iPS-derived cells. We established mouse embryonic fibroblasts (MEFs) from animals generated by a cross of two mouse lines (*Pcdh21*/Cre and Z/EG, Fig. 1a). The Z/EG transgene labels most cells in an animal with a visible marker (β-geo, a fusion of the β-galactosidase and neomycin genes)[17], whereas the *Pcdh21*/Cre modification results in Cre expression in rare neuronal subtypes, but not in ES cells[18]. Cre expression causes excision of the floxed β-geo gene, resulting in green fluorescent protein (GFP) expression in olfactory bulb mitral cells, a feature we exploit later (Fig. 1a).

We reasoned that the inappropriate expression of reprogramming genes during development could inhibit embryonic and postnatal development. Therefore, we designed a drug-inducible lentiviral reprogramming strategy to achieve tight control of transgene expression in iPS cells and their derivatives (Fig. 1b)[19]. The four original reprogramming factors (*Oct4* (also known as *Pou5f1*), *Sox2*, *Klf4* and *c-Myc*) were placed under control of the tetO promoter, which is activated by the reverse tetracycline transactivator (rtTA) protein in the presence of the tetracycline analogue doxycycline (dox). We used an enhanced version of the rtTA transcriptional activator protein (rtTAM2.2) that induces higher gene expression levels than the rtTAM2 protein[20]. To promote complete reprogramming and to facilitate isolation of fully reprogrammed iPS cells we exposed MEFs to the histone deacetylase inhibitor valproic acid (VPA), which has been reported to enhance reprogramming efficiency and to select against incompletely reprogrammed cells by inhibiting cell division[21,22] (see Methods).

Reprogramming of *Pcdh21*/Cre–Z/EG fibroblasts by this method resulted in ES-cell-like colonies after five (with dox plus VPA) to seven (dox only) days of dox induction (Fig. 1c, d and Methods). No colonies emerged in the absence of dox, which demonstrates both the inducibility and specificity of our system. We subcloned 21 colonies from the dox-plus-VPA-treated cells, which we refer to as iMZ iPS cell lines.

At present, there is no established method to select iPS cells that will contribute to all of the tissues of an organism. To prioritize the iMZ cell lines for tetraploid complementation assays, we assessed lines for similarity to ES cells by morphology, proliferation rate, expression of pluripotency markers and ability to generate embryoid bodies (Figs 1d, 2d and Supplementary Figs 2 and 3). We also exploited our cell-type-specific Cre line to determine whether embryoid bodies made from our iMZ lines could generate cells that resembled olfactory bulb mitral cells on the basis of neuronal morphology and GFP expression (Fig. 1e and Supplementary Fig. 3). Using these criteria, we selected 12 candidate lines for karyotype analysis (Supplementary Figs 4, 5 and Methods). To establish the pluripotency of lines

[1]Department of Cell Biology, [2]Mouse Genetics Core Facility, The Scripps Research Institute, 10550 North Torrey Pines Road, La Jolla, California 92037, USA. [3]Medical Scientist Training Program, University of California, San Diego, La Jolla, California 92037, USA.
*These authors contributed equally to this work.

LETTERS

Linking the p53 tumour suppressor pathway to somatic cell reprogramming

Teruhisa Kawamura[1,2]*, Jotaro Suzuki[1,3]*, Yunyuan V. Wang[1], Sergio Menendez[4], Laura Batlle Morera[4], Angel Raya[4,5,6], Geoffrey M. Wahl[1] & Juan Carlos Izpisúa Belmonte[1,4]

Reprogramming somatic cells to induced pluripotent stem (iPS) cells has been accomplished by expressing pluripotency factors and oncogenes[1–8], but the low frequency and tendency to induce malignant transformation[9] compromise the clinical utility of this powerful approach. We address both issues by investigating the mechanisms limiting reprogramming efficiency in somatic cells. Here we show that reprogramming factors can activate the p53 (also known as Trp53 in mice, TP53 in humans) pathway. Reducing signalling to p53 by expressing a mutated version of one of its negative regulators, by deleting or knocking down *p53* or its target gene, *p21* (also known as *Cdkn1a*), or by antagonizing reprogramming-induced apoptosis in mouse fibroblasts increases reprogramming efficiency. Notably, decreasing p53 protein levels enabled fibroblasts to give rise to iPS cells capable of generating germline-transmitting chimaeric mice using only Oct4 (also known as Pou5f1) and Sox2. Furthermore, silencing of p53 significantly increased the reprogramming efficiency of human somatic cells. These results provide insights into reprogramming mechanisms and suggest new routes to more efficient reprogramming while minimizing the use of oncogenes.

The p53 pathway reduces cancer initiation by inducing apoptosis or cell cycle arrest in response to a variety of stress signals, including overexpressed oncogenes such as c-Myc. Klf4 can either activate or antagonize p53, depending on the cell type used and expression level[10]. Consequently, reprogramming efficiency is probably reduced through oncogene-mediated activation of the p53 pathway. This is consistent with previous results showing that germ cells can be spontaneously reprogrammed in the absence of p53 (ref. 11), and a combination of *p53* short interfering RNA (shRNA) and Utf1 expression increased iPS cell formation[12].

We first determined whether the reprogramming factors, individually or in combination, activate the p53 pathway in mouse embryo fibroblasts (MEFs). Relative to the green fluorescent protein (GFP)-retroviral control, c-Myc considerably increased p53 abundance and activity, manifested by increased expression of the cyclin-dependent kinase inhibitor p21 (Fig. 1a). This was achieved by induction of $p19^{Arf}$, an antagonist of Mdm2, the E3-ubiquitin ligase principally responsible for p53 degradation[13]. Increased p21 protein levels were also observed in MEFs infected with Klf4 alone, with Oct4 and Sox2 (two factors) or with Oct, Sox2 and Klf4 (three factors) (Fig. 1a). Because introducing reprogramming factors increased γ-H2ax (also known as γ-H2afx) foci (Supplementary Fig. 1), we infer that the expression of reprogramming factors may induce p53 activity by DNA damage. We also compared p53 and p21 expression in a variety of mouse and human cell lines previously used for iPS cell production (Supplementary Fig. 2). Interestingly, keratinocytes, which have higher reprogramming efficiency, display lower p53 and p21 protein levels than other cell types. Moreover, p21 induction in keratinocytes is lower than in fibroblasts after infection with the three factors (Supplementary Fig. 3). Together, these data indicate that the p53 pathway is one determinant of reprogramming efficiency.

We therefore tested the effects of reducing p53 signalling by determining reprogramming efficiencies in cells in which p53 function was reduced by shRNA or ablated by homologous recombination. Most cells were infected with shRNA (Supplementary Fig. 4), p53 messenger RNA and protein levels were reduced by 60–80% (Fig. 1c and Supplementary Fig. 5), and iPS cell colony formation was increased by 2–4-fold using two different shRNAs (Fig. 1b, c). This probably underestimates p53 suppressive capacity, because functional p53 protein clearly remained present, as indicated by the ability of the p53 activating agent Nutlin-3a (ref. 14) to dose-dependently reduce iPS cell formation in MEFs treated with the most effective *p53* shRNA (Fig. 1d). In contrast, reprogramming efficiency was increased by at least tenfold in *p53*-null MEFs, and this was not reduced by Nutlin-3a (Supplementary Table 1 and Fig. 1e, g). $p53^{+/-}$ heterozygous MEFs also exhibited higher three-factor-reprogramming efficiency than wild-type MEFs. Although culture stress can induce cellular senescence and activate p53, which would reduce reprogramming, less than 1% of the cells of all p53 genotypes stained with the senescence marker β-galactosidase (Supplementary Fig. 6). Because we did not detect loss of heterozygosity of the *p53* gene in iPS cell colonies derived from $p53^{+/-}$ MEFs (Supplementary Fig. 7), the data suggest a p53 dosage-sensitivity to reprogramming (Fig. 1e). We were concerned that because *p53*-null MEFs are genetically unstable, increased reprogramming efficiency might result from expression of the three factors in variant cells. However, we found that re-expressing p53 protein in the *p53*-null MEFs markedly reduced reprogramming efficiency (Fig. 1f).

Reducing factors downstream of p53 also increased reprogramming efficiency. For example, *p21* shRNA increased reprogramming by approximately threefold (Fig. 1h). This probably underestimates the magnitude to which p21 induction suppresses reprogramming as *p21*-shRNA-expressing cells still responded to Nutlin-3a treatment as discussed earlier. We also noted a modest induction of the pro-apoptotic factor Bax, another p53-inducible gene[15], in three-factor experiments (data not shown). Consistent with a limiting role of the p53-induced apoptotic response during reprogramming, over-expression of the Bax antagonist Bcl2 suppressed apoptosis in two, three and four factor experiments, and increased the frequency of colonies expressing the pluripotency factor Nanog by fourfold

[1]Gene Expression Laboratory, Salk Institute for Biological Studies, 10010 North Torrey Pines Road, La Jolla, California 92037, USA. [2]Career-Path Promotion Unit for Young Life Scientists, Kyoto University, Kyoto 606-8501, Japan. [3]Drug Discovery Research, Astellas Pharma Inc., Tsukuba, Ibaraki 305-8585, Japan. [4]Center of Regenerative Medicine in Barcelona, Dr. Aiguader 88, 08003 Barcelona, Spain. [5]Institució Catalana de Recerca i Estudis Avançats (ICREA), Passeig Lluís Companys 23, 08010 Barcelona, Spain. [6]Networking Center of Biomedical Research in Bioengineering, Biomaterials and Nanomedicine (CIBER-BBN), Dr. Aiguader 88, 08003 Barcelona, Spain.
*These authors contributed equally to this work.

LETTERS

A genetically encoded photoactivatable Rac controls the motility of living cells

Yi I. Wu[1,3], Daniel Frey[4], Oana I. Lungu[1,2,3], Angelika Jaehrig[1,3], Ilme Schlichting[4], Brian Kuhlman[2,3] & Klaus M. Hahn[1,3]

The precise spatio-temporal dynamics of protein activity are often critical in determining cell behaviour, yet for most proteins they remain poorly understood; it remains difficult to manipulate protein activity at precise times and places within living cells. Protein activity has been controlled by light, through protein derivatization with photocleavable moieties[1] or using photoreactive small-molecule ligands[2]. However, this requires use of toxic ultraviolet wavelengths, activation is irreversible, and/or cell loading is accomplished via disruption of the cell membrane (for example, through microinjection). Here we have developed a new approach to produce genetically encoded photoactivatable derivatives of Rac1, a key GTPase regulating actin cytoskeletal dynamics in metazoan cells[3,4]. Rac1 mutants were fused to the photoreactive LOV (light oxygen voltage) domain from phototropin[5,6], sterically blocking Rac1 interactions until irradiation unwound a helix linking LOV to Rac1. Photoactivatable Rac1 (PA-Rac1) could be reversibly and repeatedly activated using 458- or 473-nm light to generate precisely localized cell protrusions and ruffling. Localized Rac activation or inactivation was sufficient to produce cell motility and control the direction of cell movement. Myosin was involved in Rac control of directionality but not in Rac-induced protrusion, whereas PAK was required for Rac-induced protrusion. PA-Rac1 was used to elucidate Rac regulation of RhoA in cell motility. Rac and Rho coordinate cytoskeletal behaviours with seconds and submicrometre precision[7,8]. Their mutual regulation remains controversial[9], with data indicating that Rac inhibits and/or activates Rho[10,11]. Rac was shown to inhibit RhoA in mouse embryonic fibroblasts, with inhibition modulated at protrusions and ruffles. A PA-Rac crystal structure and modelling revealed LOV–Rac interactions that will facilitate extension of this photoactivation approach to other proteins.

Recent NMR studies revealed the mechanism of a protein light switch in *Avena sativa* phototropin1 (refs 6, 12): a flavin-binding LOV2 domain interacts with a carboxy-terminal helical extension (Jα) in the dark. Photon absorption leads to formation of a covalent bond between Cys 450 and the flavin chromophore, causing conformational changes that result in dissociation and unwinding of the Jα helix. We fused the complete LOV2-Jα sequence (404–547) to the amino terminus of a constitutively active Rac1, anticipating that the LOV domain in its closed conformation would block the binding of effectors to Rac1, and that light-induced unwinding of the Jα helix would release steric inhibition, leading to Rac1 activation (Fig. 1a). Sampling of different junctional sequences in pull-down assays revealed that connecting Leu 546 of LOV2-Jα to Ile 4 of Rac1 led to substantial reduction in Rac1 binding to its effector PAK (Fig. 1b and Supplementary Fig. 1a). To ensure that the photoactivatable Rac1 would induce no dominant-negative effects and that its activity would not be subject to upstream regulation, mutations were introduced to abolish GTP hydrolysis and diminish interactions with nucleotide exchange factors, guanine nucleotide dissociation inhibitors (Q61L) and GTPase activating proteins (E91H and N92H) (Supplementary Fig. 2 and Supplementary text 'Characterization of Rac1 constructs'). This resulted in the photoactivatable analogue of Rac1 (PA-Rac1) used in the following studies. Pull-down assays showed that PA-Rac1 has greatly reduced affinity for its effector protein PAK in the dark, as does a PA-Rac1 construct containing a light-insensitive LOV2 mutation (C450A)[13]. Effector binding was restored in a PA-Rac1 construct containing a LOV2 mutant (I539E)[14] which mimics the unfolded 'lit state' (Fig. 1b and Supplementary Fig. 1b). Isothermal titration experiments indicated that the dark and lit state mutants of PA-Rac1 differed tenfold in effector binding (200 nM versus 2 μM) (Supplementary Fig. 3 and Supplementary Table 1), with lit state effector affinity similar to that of native Rac[15].

Activation of PA-Rac1 was examined in HeLa cells expressing a YFP fusion of PA-Rac1 to gauge expression level. The cells remained quiescent when illuminated with wavelengths longer than flavin absorbance (515, 568 or 633 nm, data not shown), but within seconds after switching to 458 nm, lamellipodial protrusions and membrane ruffles appeared around the cell edges (Fig. 1c and Supplementary Movie 1). To show that this effect was due to PA-Rac1, kymograms were used to quantify maximum protrusion length; irradiation of PA-Rac1 elicited protrusions that were four times as long as those seen in cells expressing either LOV domain alone or the light-insensitive PA-Rac1(C450A) mutant (Supplementary Fig. 4). An important advantage of PA-Rac1 is its ability to control precisely the subcellular location of Rac activation. We first examined this in mouse embryo fibroblasts (MEFs) stably expressing PA-Rac1, and cultured without serum to minimize cell activity before irradiation. Irradiation of 20-μm spots at the cell edge generated large protrusions clearly localized next to the point of irradiation (Fig. 1d and Supplementary Movie 2). Repeated irradiation led first to ruffles and then to protrusion. YFP–actin, YFP–PAK and YFP–Arp3 revealed actin polymerization at the edge of the Rac-induced protrusions with associated translocation of downstream effectors, and induction of localized PAK phosphorylation was shown by immunostaining (Supplementary Figs 5 and 6 and Supplementary Movies 3 and 4). Movement of a laser spot to different positions led to cessation of ruffling or protrusion at the initial irradiation position and new activities appearing where the laser spot was brought to rest (HeLa cells, Supplementary Movie 5), demonstrating reversible activation. In MEF cells, more prone to movement than HeLa cells, complex shape changes were produced by 'painting' the cell with the laser spot (Supplementary Movie 6). The area of protrusions in MEF cells was dependent on light dosage, indicating the valuable ability to control the level of Rac1 activation (Supplementary Fig. 7). PA-Rac1 diffusion was analysed using fluorescence recovery after photobleaching (FRAP) and using PA-Rac1 tagged with photoactivatable GFP[16] (Supplementary

[1]Department of Pharmacology, [2]Department of Biochemistry and Biophysics, and [3]Lineberger Comprehensive Cancer Center, University of North Carolina, Chapel Hill, North Carolina 27599, USA. [4]Department of Biomolecular Mechanisms, Max Planck Institute for Medical Research, Jahn-Strasse 29, 69120 Heidelberg, Germany.

Isolation of deletion alleles by G4 DNA-induced mutagenesis

Daphne B Pontier[1,2], Evelien Kruisselbrink[1,2], Victor Guryev[1] & Marcel Tijsterman[1,2]

Metazoan genomes contain thousands of sequence tracts that match the guanine-quadruplex (G4) DNA signature $G_3N_xG_3N_xG_3N_xG_3$, a motif that is intrinsically mutagenic, probably because it can form secondary structures during DNA replication. Here we show how and to what extent this feature can be used to generate deletion alleles of many *Caenorhabditis elegans* genes.

The ability of DNA sequences to form structures other than canonical Watson-Crick duplexes is potentially dangerous for the faithful segregation of genetic information. Such structures may form during processes that involve transient denaturation of the DNA duplex, such as DNA replication, transcription or DNA repair[1]. Thermodynamically stable secondary structures could impede the progression of DNA and RNA polymerases[2,3], and it has been suggested that specialized proteins exist that resolve or repair such structural impediments. One structure that readily forms *in vitro* in guanine-rich DNA is guanine-quadruplex DNA (G4 DNA)[4,5]: guanine-rich ssDNA can adopt a four-stranded configuration, which consists of square arrangements of guanines, stabilized by Hoogsteen hydrogen bonding (**Fig. 1a**). After observations that poly(G) tracts are deleted in *C. elegans* strains with mutations in the DNA helicase *dog-1*, the ortholog of the human Fanconi J (*FANCJ*, also known as *BRIP1*) gene[6,7], we recently showed that G4 DNA is mutagenic in this genetic background *in vivo*[8]. We found that the G4 DNA signature $G_3N_xG_3N_xG_3N_xG_3$, where N is any nucleotide, is the best predictor of *dog-1*–dependent mutagenicity[8]. Array comparative genome hybridization analysis of so-called mutator accumulation lines (worms were clonally grown for ten generations, allowing DNA replication errors to accumulate) had demonstrated that G4 DNA sequences can be deleted in germ nuclei at very high frequency[8]. One specific guanine tract had been lost in 3 of 16 *dog-1* substrains after just ten generations of growth[8]. Such great extent of site-specific mutagenesis suggests that deletion alleles of genes that flank a G4 DNA site can be isolated in populations of *dog-1* worms. Here we describe the methodology to do so, provide proof of principle by isolating deletion alleles in various genes and list all *C. elegans* G4 DNA sites for researchers to inspect whether their genes of interest are close to one of these sites.

We identified 2,907 sites in the *C. elegans* genome that matched the G4 DNA signature $G_{3+}N_{1-7}G_{3+}N_{1-7}G_{3+}N_{1-7}G_{3+}$ (four stretches of at least three consecutive guanines, alternated with 1–7 nucleotides of any kind). We named these sites *qua* or *ggg 1–2907*, where ggg refers to homoguanine tracts and qua to non-homoguanine G4 DNA. Increasing tract length and G-richness may increase the probability of G4 DNA formation, and we thus ranked these endogenous sites according to the number of possible different G4 DNA configurations. As an example, there is only one way to fold *qua129*, GGGTGGGAGGGAGGG, into a four-stranded configuration with three planar guanine quartets (with one nucleotide in the loop), whereas there are 83 different ways to fold *qua1442*, GGG AGGGGGTGGGGGAGGGGGGGG, into a structure with three guanine quartets. According to this rationale, a homoguanine tract of similar size ranks very high.

We next inspected the mutagenic potential of several of these G4 DNA sites by performing nested PCR analyses with primers that we positioned ~1 kilobase 5′ and 0.1 kilobase 3′ of the G4 sequence, as we and others have found that deleted sequences are almost exclusively positioned 5′ of the guanine tract[6,8]. We identified 3 mutagenic G4 DNA sites in which we observed (somatic) deletions in either 5 adult *dog-1* worms or in DNA isolated from populations of approximately 10,000 worms (**Fig. 1b**). We postulate that we can identify minute amounts of smaller-than-wild-type products because these preferably amplify under suboptimal PCR conditions and also because they lack the potentially replication-blocking G-rich sequence. In our analysis of whole populations by nested PCR and subsequent gel electrophoresis, we frequently observed smears instead of single bands in the gels, which we interpreted as amplification of many bands of different size. Little is known about possible mutagenic determinants in the G4 DNA structure *in vivo* (for example, loop size and number of possible planar rings), and ongoing work is aimed at addressing this in a systematic way. In this analysis we found that sites which minimally comply with the G4 DNA consensus $G_3N_xG_3N_xG_3N_xG_3$ are mutagenic *in vivo* (**Fig. 1b**), which suggests that many of the predicted G4 DNA sites have deletion-forming potential.

We then searched for assay conditions that would allow us to distinguish germline deletion events (which will propagate during population growth) from somatic events. We tested at which stage of population growth a germline deletion should occur for us to identify it in a PCR-based approach. To this end, we started populations with a single wild-type Bristol N2 hermaphrodite worm (P0), allowed the populations to expand and mixed in one

[1]Hubrecht Institute–Koninklijke Nederlandse Akademie van Wetenschappen, University Medical Centre Utrecht, Utrecht, The Netherlands. [2]Present address: Department of Toxicogenetics, Leiden University Medical Center, Leiden, The Netherlands. Correspondence should be addressed to M.T. (m.tijsterman@lumc.nl).

RECEIVED 10 APRIL; ACCEPTED 22 JUNE; PUBLISHED ONLINE 16 AUGUST 2009; DOI:10.1038/NMETH.1362

PCR products as transcription templates. The production of active enzymes modified post-translationally by the addition of biotin-geranyl pyrophosphate further highlights the utility of this approach. Because the N-terminal leader of the initial SITS design extends the natural protein sequence, Mureev *et al.*[1] also demonstrate effective translation using only the upstream portion of the SITS module. These truncated SITS elements are somewhat less effective but still enable substantial product accumulation and should produce the authentic protein. Even though the new system appears to be limited to cytoplasmic proteins, it promises great utility.

For example, one of the more interesting issues to be addressed for newly sequenced organisms is to identify which proteins interact with each other or with small molecules. The extent of these interactions can indicate the occurrence—and possibly the importance—of signaling pathways and regulatory mechanisms. In this pursuit, Mureev *et al.*[1] use fluorescence correlation and cross-correlation spectroscopies[8] to demonstrate that their new system allows the real-time, *in situ* characterization of such interactions.

So what might these new advances deliver in the near future? As the authors point out, the applications are not limited to cell-free protein synthesis. For instance, mRNAs that are enabled by SITS elements could be introduced into mammalian cells using established nucleic-acid transfection procedures. The impact of the temporary overexpression of the protein would indicate its impact on signaling or other metabolic functions. This would be an excellent complement to the introduction of interfering RNAs, as both stimulatory and inhibitory nucleic acids could be introduced to simultaneously increase and decrease the levels of different proteins without requiring chromosomal modifications.

Still, the most important implications of this study are likely to be in the field of cell-free protein synthesis. The new ability to activate protein synthesis in extracts of nearly every organism offers tremendous opportunities. These methods can initially be used as a source of 'naturally' produced proteins but can then be applied to elucidating metabolic and regulatory pathways and mechanisms. For example, we recently reported methods for high-throughput evaluation of the effect of endogenous proteins on the overall process of protein synthesis and folding[9]. There are now many other methods for multiplexed gene expression and analysis, and the advances reported by Mureev *et al.*[1] promise to extend these to most organisms. Although we will still be limited primarily to the production of cytoplasmic proteins, these approaches can deliver an invaluable treasure of new knowledge and biological reagents.

1. Mureev, S., Kovtun, O., Nguyen, U.T.T. & Alexandrov, K. *Nat. Biotechnol.* **27**, 747–752 (2009).
2. Nirenberg, M.W. & Matthaei, J.H. *Proc. Natl. Acad. Sci. USA* **47**, 1588–1602 (1961).
3. Shimizu, Y. *et al. Nat. Biotechnol.* **19**, 751–755 (2001).
4. Jewett, M.C. *et al. Mol. Syst. Biol.* **4**, 220 (2008).
5. Bablanian, R. *et al. J. Virol.* **65**, 4449–4460 (1991).
6. Kamura, N. *et al. Bioorg. Med. Chem. Lett.* **15**, 5402–5406 (2005).
7. Shaloiko, L.A. *et al. Biotechnol. Bioeng.* **88**, 730–739 (2004).
8. Bacia, K. & Schwille, P. *Nat. Protocols* **2**, 2842–2856 (2007).
9. Woodrow, K.A. & Swartz, J.R. *Proteomics* **7**, 3870–3879 (2007).

Next-generation quantum dots

Andrew M Smith & Shuming Nie

Quantum dots that are small and non-blinking offer new opportunities for dynamic single-molecule imaging in live cells.

Quantum dots are brightly fluorescent nanocrystals that have found use across a broad spectrum of biological imaging applications. When observed individually under a fluorescence microscope, these particles show a rapid on-and-off 'blinking' of their emission, an attribute that is often detrimental, especially for single-molecule imaging, as the molecules being monitored exhibit frequent loss of signal. In a recent paper in *Nature*, Wang *et al.*[1] reported that quantum dots with an alloyed composition gradient from the core to the surface do not blink but rather remain continuously 'on'. This finding is both surprising and profound, and represents considerable progress toward the next generation of fluorescent intracellular probes.

Fluorescent dyes and proteins have been invaluable for visualizing the dynamics and interactions of biomolecules within living cells. Unfortunately, light emission by these tags rapidly decays during observation, and the weak intensity of the emitted light cannot be readily detected from single molecules. Single quantum dots, however, are immensely bright and easily observed using standard fluorescence microscopes, and they emit light hundreds to thousands of times longer than do fluorescent dyes and proteins. These two key characteristics have spurred intense interest in the use of these particles for live-cell imaging, but the utility of these particles has been limited, in part, because current commercially available quantum dots rapidly blink, are hydrodynamically large, are multivalent when functionalized with biological molecules and often aggregate inside cells.

Andrew M. Smith and Shuming Nie are in the Departments of Biomedical Engineering and Chemistry, Emory University and Georgia Institute of Technology, Atlanta, Georgia, USA. e-mail: snie@emory.edu

Scientists have attempted to control the blinking behavior of quantum dots for over a decade, operating under the assumption that these nanocrystals turn off when they lose electrons, that is, when they become ionized. Before the work of Wang *et al.*[1], other researchers observed that blinking can be attenuated if a quantum dot core is coated with a thick crystalline shell that electronically insulates the core to prevent ionization[2,3]. Although it is not possible to completely eliminate blinking using a thick shell, the optimized core-shell particles are in the 'on' state for >97% of the time and are never 'off' for longer than tens of milliseconds. Wang *et al.*[1] were able to completely eliminate blinking by preparing core-shell particles in which there is a smooth composition gradient from the core to the shell, a structure that never blinks because it can emit light when it is ionized (**Fig. 1**). A crucial difference between the thick-shell and gradient structures is the overall size of the resulting nanocrystals. Growth of a thick shell structure invariably leads to large quantum dots (generally >13 nm), whereas the particles with a gradient structure can be produced at a more compact size of 5–7 nm.

The hydrodynamic size of a nanoparticle probe has a large impact on its behavior in cellular environments. This is especially true for intracellular applications, as the cellular cytoplasm is a crowded maze of macromolecular structures that act as a sieve to limit diffusion of large molecules. Experiments with polysaccharides suggest that the cytoplasmic diffusion in a cell of a molecule larger than ~15 nm in diameter is a small fraction of its mobility in aqueous solution, and a particle as large as 50 nm is effectively immobile[4]. Current quantum dots are generally 15–35 nm in diameter, with an elongated shape, and fall well within the range of strongly limited mobility[5]. Interestingly, on the other end of the spectrum, particles that are exceptionally small (<3 nm) may be

nature biotechnology

Species-independent translational leaders facilitate cell-free expression

Sergei Mureev[1], Oleksiy Kovtun[1], Uyen T T Nguyen[2] & Kirill Alexandrov[1,2]

Cell-free protein synthesis enables the rapid production and engineering of recombinant proteins. Existing cell-free systems differ substantially from each other with respect to efficiency, scalability and the ability to produce functional eukaryotic proteins. Here we describe species-independent translational sequences (SITS) that mediate efficient cell-free protein synthesis in multiple prokaryotic and eukaryotic systems, presumably through bypassing the early translation initiation factors. We use these leaders in combination with targeted suppression of the endogenous *Leishmania tarentolae* mRNAs to create a cell-free system based on this protozoan. The system can be directly programmed with unpurified PCR products, enabling rapid generation of large protein libraries and protein variants. *L. tarentolae* extract can produce up to 300 μg/ml of recombinant protein in 2 h. We further demonstrate that protein-protein and protein–small molecule interactions can be quantitatively analyzed directly in the translation mixtures using fluorescent (cross-) correlation spectroscopy.

Cell-free protein expression systems have been invaluable in studies of protein translation mechanisms, protein engineering and interactions, *in vitro* evolution and structural research[1,2]. The best characterized and most widely used cell-free translation systems are based on *Escherichia coli*, one of which (PURE) exclusively comprises recombinant components[3]. The main shortcomings of *E. coli*–based cell-free systems are the lack of chaperone-based mechanisms needed to fold complex eukaryotic proteins and the absence of post-translational modifications specific to eukaryotes. Eukaryotic cell-free systems based on wheat germ extract (WGE), rabbit reticulocyte lysate (RRL) and insect cell extract (ICE) overcome some of these problems[4–6]. Their ability to couple transcription and translation reactions on PCR-generated templates in multiplexed format greatly simplifies and accelerates protein production. This methodology has been used for protein engineering and production of protein arrays for many applications including drug screening and diagnostics (for review, see ref. 7). However, these eukaryotic cell-free systems do not scale up or down easily, are laborious and expensive to prepare, and are derived from source organisms that are difficult to manipulate genetically. Large batch-to-batch variation is also inevitable because of the long life cycle of the host organisms subject to many environmental influences. An alternative system based on a rapidly growing, fermentable organism that is amenable to technically straightforward genetic modifications is therefore highly desirable.

Three main obstacles must be overcome to create an efficient cell-free expression system. First, the system has to be programmed with exogenous mRNA that can efficiently engage the translational machinery. Second, endogenous mRNAs must be degraded or otherwise prevented from being translated. Finally, practical protocols must be developed for preparing cell-free extracts that retain a functional translational apparatus. The biggest hurdle of cell-free protein synthesis is reprogramming the system with exogenous mRNA. Although the problem is readily solved in an *E. coli*–based system by using natural or synthetic ribosome binding sites, it presents a substantial challenge in eukaryotic systems where assembly of the translational complex requires a 5′-capped mRNA and numerous translational factors[8,9]. As cell-free expression systems typically use RNA that is synthesized *in vitro* and is therefore uncapped, they fail to engage the cap-binding complex and early translation factors that are required to form the 43S preinitiation complex. The problem is partially overcome by enzymatic *in vitro* capping or by using cap-independent untranslated regions (UTRs), which mimic the cap structure and promote ribosomal complex assembly on the mRNA[10,11]. However, context dependence and species specificity of the latter sequences often complicate their generic application.

Undesired background translation is often prevented by digesting the endogenous mRNAs with micrococcal nuclease, which is more active toward mRNA than toward the ribonucleoprotein translational complexes. However, the inevitable partial degradation of tRNAs and rRNAs by such treatment reduces the translational activity of the lysate[12], making alternative strategies highly desirable.

We describe the design of species-independent, universal translation-initiation leaders that engage ribosomes directly and thereby bypass the cap-dependent pathway. We used these leaders to develop a eukaryotic cell-free system based on extracts of the protozoan *L. tarentolae*.

RESULTS

Development of a universal translation-initiating sequence

Ribosomes comprise an evolutionarily conserved catalytic core of translation machinery. This core has been extended in eukaryotes by a large array of translation initiation factors. RNA secondary

[1]Institute for Molecular Bioscience and Australian Institute for Bioengineering and Nanotechnology, The University of Queensland, Brisbane, Queensland, Australia. [2]Max-Planck-Institute for Molecular Physiology, Dortmund, Germany. Correspondence should be addressed to K.A. (k.alexandrov@uq.edu.au).

Received 5 June; accepted 6 July; published online 2 August 2009; doi:10.1038/nbt.1556

nature biotechnology

Stabilized gene duplication enables long-term selection-free heterologous pathway expression

Keith E J Tyo, Parayil Kumaran Ajikumar & Gregory Stephanopoulos

Engineering robust microbes for the biotech industry typically requires high-level, genetically stable expression of heterologous genes and pathways. Although plasmids have been used for this task, fundamental issues concerning their genetic stability have not been adequately addressed. Here we describe chemically inducible chromosomal evolution (CIChE), a plasmid-free, high gene copy expression system for engineering *Escherichia coli*. CIChE uses *E. coli recA* homologous recombination to evolve a chromosome with ~40 consecutive copies of a recombinant pathway. Pathway copy number is stabilized by *recA* knockout, and the resulting engineered strain requires no selection markers and is unaffected by plasmid instabilities. Comparison of CIChE-engineered strains with equivalent plasmids revealed that CIChE improved genetic stability approximately tenfold and growth phase–specific productivity approximately fourfold for a strain producing the high metabolic burden–biopolymer poly-3-hydroxybutyrate. We also increased the yield of the nutraceutical lycopene by 60%. CIChE should be applicable in many organisms, as it only requires having targeted genomic integration methods and a *recA* homolog.

Recent breakthroughs in metabolic engineering have made it easier to overproduce biochemical products from renewable resources. Such advances include fabricating large synthetic pathways (*de novo* synthesized DNA sequences)[1,2] and optimizing pathway expression through transcription- or translation-level engineering[3,4], which is essential to avoid buildup of toxic products. This progress has relied mainly on plasmid-based gene expression or single-copy genomic integration.

Although plasmids are easy to insert into a cell and allow strong gene expression, they suffer from genetic instability due to three processes that reduce the number of active recombinant alleles in a culture[5]: (i) segregational instability, in which unequal distribution of plasmids to daughter cells results in plasmid-free cells; (ii) structural instability, in which some plasmids contain an altered DNA sequence that causes incorrect expression of the desired proteins; and (iii) allele segregation, in which productive plasmids are displaced by nonproductive plasmids, leading to nonproductive cells that are resistant to selection pressure.

Whereas various strategies have been implemented to reduce segregational and structural instability[6], allele segregation, which is not mitigated by selection markers or post-segregational killing mechanisms (PSK), has not been considered as a potential mechanism for productivity loss in biotechnology. Even so, it is likely that allele segregation has affected many pathway-engineering efforts by decreasing product yield and productivity of the desired chemical in batch or continuous fermentation. This unaddressed plasmid problem is ubiquitous in industrial biotechnology and will likely affect future endeavors to produce bioproducts using minimal-genome cells[7].

These three sources of instability suggest that the stable expression of genetic constructs through *de novo* chromosomal engineering, rather than artificial plasmid-based systems, is much needed to advance microbial overproduction using heterologous pathways. Here we present such a technique, CIChE, for biosynthetic pathway engineering in microbial hosts (**Fig. 1**) to circumvent allele segregation, a fundamental flaw in plasmid-based gene expression (**Fig. 2**). We use a mathematical model to explain that random plasmid inheritance, rather than mutation rates, drives productivity loss, whereas ordered inheritance, such as CIChE, can stabilize pathway productivity tenfold longer. We also demonstrate that CIChE allows cells with heavy metabolic burdens to remain productive and maintain or increase yields for many more generations than do analogous plasmid constructs. These results open the possibility for the broad use of CIChE-engineered microbes in large-scale industrial production.

RESULTS

Random distribution, not mutation rates, limit the genetic stability of plasmids

Although structural and segregational instability have been understood for some time[5], strategies devised to mitigate these instabilities, such as selection markers and post-segregational killing mechanisms, can maintain active plasmids for only ~35 generations (an example of plasmid productivity loss in the presence of antibiotics is presented later). This loss in productivity is too rapid to be explained by mutation alone because mutations in all copies of the plasmid should not accumulate fast enough. If antibiotics were used to maintain selection pressure, this phenomenon could not be explained by structural or segregational instability.

Allele segregation, in contrast, can explain how a rare initial mutation can be rapidly propagated in a culture, decreasing productivity regardless of mutation rate. The logic is as follows: because recombinant pathways typically place heavy metabolic burdens on the cell

Department of Chemical Engineering, Massachusetts Institute of Technology, Cambridge, Massachusetts, USA. Correspondence should be addressed to G.S. (gregstep@mit.edu).

Received 31 March; accepted 29 June; published online 26 July 2009; doi:10.1038/nbt.1555

Fluctuating hydrodynamics and microrheology of a dilute suspension of swimming bacteria

A. W. C. Lau
Department of Physics, Florida Atlantic University, Boca Raton, Florida 33431, USA

T. C. Lubensky
Department of Physics and Astronomy, University of Pennsylvania, Philadelphia, Pennsylvania 19104, USA

(Received 11 February 2009; published 22 July 2009)

A bacterial bath is a model active system consisting of a population of rodlike motile or self-propelled bacteria suspended in a fluid environment. This system can be viewed as an active, nonequilibrium version of a lyotropic liquid crystal or as a generalization of a driven diffusive system. We derive a set of phenomenological equations, which include the effects of internal force generators in the bacteria, describing the hydrodynamic flow, orientational dynamics of the bacteria, and fluctuations induced by both thermal and nonthermal noises. These equations violate the fluctuation dissipation theorem and the Onsager reciprocity relations. We use them to provide a quantitative account of results from recent microrheological experiments on bacterial baths.

DOI: 10.1103/PhysRevE.80.011917 PACS number(s): 87.18.Hf, 05.40.−a, 87.10.−e

I. INTRODUCTION

Many species of bacteria, such as *E. coli*, are rodlike, single-celled organisms that actively navigate their environment by swimming [1]. A common mechanism for motility is based on the rotation of bacterial flagella propelled by the action of rotary motors embedded in the cell wall. When all the motors rotate counterclockwise, the flagella bundle up and propel a bacterium forward in the direction of its long axis. This is called "run." When some of the flagella rotate clockwise, the flagella unbundle and the cell body spins or "tumbles." On average, a bacterium tumbles for about 0.1 s before it "runs" in a different (random) direction; the typical run time is about 1 s. Therefore, at long time, a bacterium appears to perform a sort of random walk [2,3]. With a typical size of a bacterium of the order of microns and a typical speed of the order of 10 μm/s, the Reynolds number $\mathcal{R}$ is much less than 1.

Early experimental studies utilizing light-scattering technique demonstrated that the velocity distribution of motile microorganisms, in general, and bacteria, in particular, is not Maxwellian [4], indicating that their motion is far more complex than that of Brownian particles [5]. A large concentration of these microorganisms constitutes a state that is far from equilibrium, exhibiting self-organized collective motion with spatial and temporal patterns such as swirls and jets [6–11].

More quantitative information about a bacterial bath (e.g., of *E. coli*) can be extracted from microrheological measurements, which track the motion of passive micron-sized beads dispersed in it [6,7,12]. Interestingly, the mean-squared displacement (MSD) of these passive beads is superdiffusive at short time and diffusive at long time, with a diffusion constant that is a few orders of magnitude greater than that of the same beads in water. These studies of the microrheology of bacterial baths clearly demonstrate that the motility of bacteria drastically alters the physical properties, i.e., response and fluctuations of the fluid environment in which they are suspended. The phenomena of superdiffusion and self-organized behaviors have been either observed or predicted in other active systems as well [13–20].

The experiments on baths of *E. coli* [6,7,12] cited above did not address the violation of the fluctuation-dissipation theorem (FDT), the effects of spatial heterogeneities in the bath, or the effects of different bacterial swimming modes. These issues are crucial to a consistent interpretation of microrheological experiments in active systems in general and in bacterial baths in particular [14] (see also Appendix A). They were addressed in a recent experimental study by *Chen et al.* [21]. In that study, two strains of *E. coli*, a rod-shaped bacterium with dimensions 3×1 μm, were used: one strain is the wild type, which tumbles and runs, and the other is the tumbler, which predominantly tumbles. In contrast to previous experiments, these experiments [21] carried out simultaneous measurements of both one- and two-point passive microrheology. One-point measurements are sensitive to the local environment of the probe colloidal particle. Two-point measurements, on the other hand, automatically average over system inhomogeneities and provide an unambiguous measure of the parameters characterizing bulk rheological properties [14,22]. The Chen study [21] also carried out independent measurements of the response of beads in the bath to controlled external forces and from it extracted the effective viscosity of the bath. The results of this study are that, even at low bacterial volume fraction ($\phi\sim10^{-3}$), fluctuations in the bath are considerably enhanced over those of pure water and that tracer particles exhibit superdifussive behavior, even though the viscosity of the bath was indistinguishable from that of water. This indicates that FDT is strongly violated and, thus, that a bacterial bath is a far-from-equilibrium system. The Chen experiments found in addition that, for the wild-type bacteria, MSDs extracted from one- and two-point measurements are different, providing strong evidence that spatial heterogeneities, possibly in the form of vortices and spirals, are present. For the tumblers, the power spectrum, $\Delta(\omega)$, was found to be Lorentzian, whereas for the wild type, it was found to scale with frequency ω as $\Delta(\omega)\sim\phi/\sqrt{\omega}$. These stress fluctuations, whose functional form is different from that of thermal fluctuations, arise from the active process of tumbling or swimming of bacteria. The purpose of this paper is to derive the long-wavelength low-frequency

Self-organization of the MinE protein ring in subcellular Min oscillations

Julien Derr,[1,2,*] Jason T. Hopper,[1] Anirban Sain,[3] and Andrew D. Rutenberg[1,†]
[1]*Department of Physics and Atmospheric Science, Dalhousie University, Halifax, Nova Scotia, Canada B3H 3J5*
[2]*FAS Center for Systems Biology, Northwest Labs, Harvard University, 52 Oxford Street, Cambridge, Massachusetts 02138, USA*
[3]*Department of Physics, Indian Institute of Technology–Bombay, Powai 400076, India*
(Received 1 August 2008; revised manuscript received 11 May 2009; published 27 July 2009)

We model the self-organization of the MinE ring that is observed during subcellular oscillations of the proteins MinD and MinE within the rod-shaped bacterium *Escherichia coli*. With a steady-state approximation, we can study the MinE ring generically—apart from the other details of the Min oscillation. Rebinding of MinE to depolymerizing MinD-filament tips controls MinE-ring formation through a scaled cell shape parameter $\tilde{r}$. We find two types of E-ring profiles near the filament tip: either a strong plateaulike E ring controlled by one-dimensional diffusion of MinE along the bacterial length or a weak cusplike E ring controlled by three-dimensional diffusion near the filament tip. While the width of a strong E ring depends on $\tilde{r}$, the occupation fraction of MinE at the MinD-filament tip is saturated and hence the depolymerization speed does not depend strongly on $\tilde{r}$. Conversely, for weak E rings both $\tilde{r}$ and the MinE to MinD stoichiometry strongly control the tip occupation and hence the depolymerization speed. MinE rings *in vivo* are close to the threshold between weak and strong, and so MinD-filament depolymerization speed should be sensitive to cell shape, stoichiometry, and MinE-rebinding rate. We also find that the transient to MinE-ring formation is quite long in the appropriate open geometry for assays of ATPase activity *in vitro*, explaining the long delays of ATPase activity observed for smaller MinE concentrations in those assays without the need to invoke cooperative MinE activity.

DOI: 10.1103/PhysRevE.80.011922 PACS number(s): 87.17.Ee, 87.16.A−, 87.16.dr

I. INTRODUCTION

The oscillation of the proteins MinD and MinE from pole to pole of individual cells of the bacterium *Escherichia coli* is used to localize cellular division to midcell [1]. One cycle of the oscillation, lasting approximately 1 min, starts with adenosine triphosphate (ATP)-associated MinD binding to the bacterial inner membrane and polymerizing into helical filaments [2–4] (see also [5]). This occurs at alternating poles of the bacterium, with the MinD forming a polar "cap." MinE is recruited to the membrane-bound MinD, where it forms a distinctive "E ring" [6–8] at the edge of the MinD cap by accumulating near the MinD-filament tips [2]. Because the rate of hydrolysis and subsequent release of ATP MinD is stimulated by MinE [3,4,9], the E ring drives depolymerization of the MinD filament which allows the oscillation to proceed. The depolymerization occurs with an approximately fixed E-ring width and speed along the cell axis [7,8], indicating an approximate steady state during this part of the Min oscillation. However, little is known about the mechanism of E-ring formation, its detailed structure, or how important it is for Min oscillations. Indeed, Min oscillations have been observed without prominent E rings [10].

Most models proposed for Min oscillation do not have explicit MinD filaments [11–15], though they do have E rings. Recently, several models of Min oscillations that include explicit MinD polymerization have been proposed [16–19], two of which display strong E rings that track the tips of depolymerizing MinD-filament caps with constant speed and width [18,19]. In these models, E rings are the result of MinE polymerization either orthogonal to [18] or along [19] MinD filaments. While MinD polymerization has been observed *in vitro* [3,4], there have been no reports of MinE polymerization in the experimental literature. Indeed, the faint MinE "zebra stripes" associated with the MinD zones adjacent to the MinE ring [7,8,10] seem to imply sparse lateral binding of MinE to the body of MinD filaments—not MinE polymerization.

In this paper, with both stochastic three-dimensional (3D) simulations and a deterministic one-dimensional (1D) model, we show that local (nonpolymeric) rebinding of MinE released from depolymerizing MinD-filament tips is sufficient for E-ring formation. We impose and characterize a dynamical steady state of an E ring on a depolymerizing semi-infinite MinD filament in order to address the approximate steady-state speed and width of the E ring *in vivo* [7,8]. We investigate the roles of spatial dimension, cell length, radius, and multiple MinD filaments and their helical pitch. We estimate the time scale of E-ring formation and obtain results consistent with the significant delay before ATPase activity seen with small MinE concentrations and large MinD membrane coverage *in vitro* [3,4]. Finally, we discuss how competition between the intrinsic and the MinE-stimulated ATPase activity of MinD controls the instability that leads to the initial formation of the E ring from a uniformly decorated MinD filament.

Qualitatively, we predict that the width of MinE rings will increase as the MinD-filament depolymerization speed is increased through manipulation of cell shape, MinD to MinE stoichiometry, or mutations that affect the MinE binding rate to MinD. Eventually, the depolymerization speed will saturate but the E-ring width can still grow. Conversely, as the depolymerization speed is decreased, MinE rings will un-

*julien.derr@espci.org
†andrew.rutenberg@dal.ca

Stochastic kinetics of ribosomes: Single motor properties and collective behavior

Ashok Garai,[1] Debanjan Chowdhury,[1] Debashish Chowdhury,[1,*] and T. V. Ramakrishnan[2,3]
[1]*Department of Physics, Indian Institute of Technology, Kanpur 208016, India*
[2]*Department of Physics, Banaras Hindu University, Varanasi 221005, India*
[3]*Department of Physics, Indian Institute of Science, Bangalore 560012, India*
(Received 30 March 2009; revised manuscript received 4 June 2009; published 9 July 2009)

Syntheses of protein molecules in a cell are carried out by ribosomes. A ribosome can be regarded as a molecular motor which utilizes the input chemical energy to move on a messenger RNA (mRNA) track that also serves as a template for the polymerization of the corresponding protein. The forward movement, however, is characterized by an alternating sequence of translocation and pause. Using a quantitative model, which captures the mechanochemical cycle of an individual ribosome, we derive an *exact* analytical expression for the distribution of its dwell times at the successive positions on the mRNA track. Inverse of the average dwell time satisfies a "Michaelis-Menten-type" equation and is consistent with the general formula for the average velocity of a molecular motor with an unbranched mechanochemical cycle. Extending this formula appropriately, we also derive the exact force-velocity relation for a ribosome. Often many ribosomes simultaneously move on the same mRNA track, while each synthesizes a copy of the same protein. We extend the model of a single ribosome by incorporating steric exclusion of different individuals on the same track. We draw the phase diagram of this model of ribosome traffic in three-dimensional spaces spanned by experimentally controllable parameters. We suggest new experimental tests of our theoretical predictions.

DOI: 10.1103/PhysRevE.80.011908 PACS number(s): 87.16.ad

I. INTRODUCTION

Ribosome is one of the largest and most complex intracellular cyclic molecular machines [1–4] and it plays a crucial role in gene expression [5]. It synthesizes a protein molecule, which is a heteropolymer of amino-acid subunits, using a messenger RNA (mRNA) as the corresponding template; this process is called *translation* (of the genetic message). Monomeric subunits of RNA are nucleotides and triplets of nucleotides constitute a codon. The dictionary of translation relates each type of possible codon with one species of amino acid. Thus, the sequence of amino acids on a protein is dictated by the sequence of codons on the corresponding template mRNA. The polymerization of protein takes places in three stages which are identified as *initiation*, *elongation* (of the protein), and *termination*. In this paper, we focus almost exclusively on the elongation stage.

A ribosome is often treated as a molecular motor for which the mRNA template also serves as a track. In each step, it moves forward on its track by one codon by consuming chemical fuel [e.g., two guanosine triphosphate (GTP) molecules]. Simultaneously, in each step, it also elongates the protein by adding an amino acid; the correct sequence of the amino acids required for polymerizing a protein is dictated by the codon sequence on the mRNA template. Therefore, it may be more appropriate to regard a ribosome as a mobile workshop that provides a platform for operation of several tools in a well-coordinated manner. Our main aim is to predict the effects of the mechanochemical cycle of individual ribosomes, in the elongation stage, on their experimentally measurable physical properties. We first focus on the single-ribosome properties which characterize their stochastic movement on the track in the absence of inter-ribosome interactions. Then we consider the additional effects of the steric interactions of the ribosomes and those of the rates of initiation and termination of translation on the collective spatiotemporal organization of the ribosomes on a track.

The stochastic forward movement of a ribosome is characterized by an alternating sequence of pause and translocation. The sum of the durations of a pause and the following translocation defines the time of a dwell at the corresponding codon. Recently, using an ingenious method, the distribution $f(t)$ of the dwell times of a ribosome has been measured [6]. We present a systematic derivation of this distribution from a detailed kinetic theory of translation which incorporates the mechanochemical cycle of individual ribosomes.

The *exact* analytical expression for $f(t)$ which we derive here is, in general, a superposition of several exponentials. On the other hand, it has been claimed [6] that the difference of two exponentials fits the experimentally measured $f(t)$ very well. We reconcile these two observations by identifying the parameter regime where our theoretically derived $f(t)$ is, indeed, well approximated by difference of two exponentials [7–11]. Moreover, we show that $\langle t\rangle^{-1}$, inverse of the mean-dwell time, satisfies a *Michaelis-Menten-like equation* [12]. The reason for this feature of the mean-dwell time is traced to the close formal similarity between the mechanochemical cycle of a ribosome and the catalytic cycle in the Michaelis-Menten theory of enzymes [12].

The elongation of the growing protein by one amino acid is coupled to the translocation of the ribosome by one codon. Therefore, $\langle t\rangle^{-1}$ is also the average velocity $\langle V\rangle$ of a ribosome on the mRNA track. An analytical expression for the average velocity of a molecular motor, whose mechanochemical cycle is unbranched, was derived by Fisher and Kolomeisky [13] in the context of motors involved in intracellular transport of cargoes [14]. The mechanochemical

*Corresponding author; debch@iitk.ac.in

Deterministic evolutionary game dynamics in finite populations

Philipp M. Altrock* and Arne Traulsen
Emmy-Noether Group of Evolutionary Dynamics, Department of Evolutionary Ecology, Max-Planck-Institute for Evolutionary Biology, 24306 Plön, Germany
(Received 5 May 2009; published 10 July 2009)

Evolutionary game dynamics describes the spreading of successful strategies in a population of reproducing individuals. Typically, the microscopic definition of strategy spreading is stochastic such that the dynamics becomes deterministic only in infinitely large populations. Here, we present a microscopic birth-death process that has a fully deterministic strong selection limit in well-mixed populations of any size. Additionally, under weak selection, from this process the frequency-dependent Moran process is recovered. This makes it a natural extension of the usual evolutionary dynamics under weak selection. We find simple expressions for the fixation probabilities and average fixation times of the process in evolutionary games with two players and two strategies. For cyclic games with two players and three strategies, we show that the resulting deterministic dynamics crucially depends on the initial condition in a nontrivial way.

DOI: 10.1103/PhysRevE.80.011909 PACS number(s): 87.23.Kg, 02.50.Ga, 02.50.Le

I. INTRODUCTION

Evolutionary game dynamics results from the transfer of economic ideas to biology [1–4]. In economics, rational players try to find the best strategy to maximize their payoffs. In biology, those individuals who use the best strategy obtain the highest reproductive fitness and spread in the population.

Traditionally, evolutionary game dynamics is considered in infinitely large, well-mixed populations. This typically leads to the replicator dynamics, a system of nonlinear differential equations governing the evolutionary dynamics [5–8]. For any composition of the population, the replicator dynamics determines deterministically the direction and velocity of evolutionary dynamics. The replicator dynamics can be derived from microscopic models of strategy spreading, which are typically stochastic [9–13]. The precise definition of strategy spreading between individuals can have decisive consequences for the dynamics, in particular in structured populations [14–21].

Since microscopic models of strategy spreading are typically stochastic, evolutionary game dynamics in finite populations can only be characterized in a probabilistic way. The most important quantities are the probability that a mutant takes over a population and the average time for this process [22–25]. Different models for strategy spreading have been proposed. A popular model is to choose two players, Harry and Sally, at random and to let Harry adopt the strategy of Sally with probability given by the Fermi function, $(1+\exp[+\beta(\pi^H-\pi^S)])^{-1}$, where π^H is the payoff of Harry and π^S is the payoff of Sally [26–29]. The parameter β measures the intensity of selection. For $\beta \ll 1$, selection is weak and strategy spreading is essentially random. For $\beta \gg 1$, selection is strong and only strategies that are more successful will be imitated. For $\beta \to \infty$, the direction of the process for two strategies becomes deterministic and thus the fixation probability is either 0 or 1. However, even in this case, the process is only semideterministic as the time of fixation remains stochastic [29].

Here, we introduce a variant of the Moran process, which leads to a fully deterministic evolutionary process in finite populations under strong selection. For weak selection, we essentially recover the transition probabilities of the standard frequency-dependent Moran process under weak selection.

We describe evolutionary game dynamics in symmetric 2×2 games defined by the general payoff matrix,

$$\begin{array}{c} \\ A \\ B \end{array}\begin{array}{c} \begin{array}{cc} A & B \end{array} \\ \begin{pmatrix} a & b \\ c & d \end{pmatrix} \end{array} . \tag{1}$$

An A player will obtain a when playing against another A or b when playing against B. Choosing strategy B results in either obtaining c (against A) or d (against B).

The average payoffs are obtained from pairwise interactions with all other individuals in the population of size N. This is the standard assumption and refers to the fact that the population is well-mixed; i.e., there is no explicit population structure. Excluding self interactions, this leads to

$$\pi_i^A = \frac{i-1}{N-1}a + \frac{N-i}{N-1}b, \tag{2}$$

$$\pi_i^B = \frac{i}{N-1}c + \frac{N-i-1}{N-1}d, \tag{3}$$

where i is the current number of A players in the population. Individuals with higher average payoffs produce offspring (or are imitated) with a higher probability. Thus, reproductive success is based on the payoff from the game. The intensity of selection β controls the importance of success in the game for reproductive success. The larger the intensity of selection, the stronger the influence of the average payoff difference on reproductive fitness.

The paper is organized in the following way. In Sec. II we introduce the birth-death process as a general framework of evolutionary dynamics between two types in finite, well-

*altrock@evolbio.mpg.de

Role of cooperative binding on noise expression

P. S. Gutierrez,[1] D. Monteoliva,[2] and L. Diambra[1,*]
[1]*Laboratorio de Biología de Sistemas, CREG–UNLP, Av. Calchaqui Km 23.5, CP 1888, Florencio Varela, Argentina*
[2]*Instituto de Física, UNLP, C.C. 67, CP 1900 La Plata, Argentina*
(Received 19 February 2009; published 22 July 2009)

The origin of stochastic fluctuations in gene expression has received considerable attention recently. Fluctuations in gene expression are particularly pronounced in cellular systems because of the small copy number of species undergoing transitions between discrete chemical states and the small size of biological compartments. In this paper, we propose a stochastic model for gene expression regulation including several binding sites, considering elementary reactions only. The model is used to investigate the role of cooperativity on the intrinsic fluctuations of gene expression by means of master-equation formalism. We found that the Hill coefficient and the level of noise increase as the interaction energy between activators increases. Additionally, we show that the model allows one to distinguish between two cooperative binding mechanisms.

DOI: 10.1103/PhysRevE.80.011914 PACS number(s): 87.18.Cf, 87.18.Tt, 87.16.Yc, 87.16.dj

I. INTRODUCTION

All chemical reactions have intrinsic fluctuations that are inversely proportional to the system size. Such fluctuations are particularly pronounced in gene expression. At the transcriptional level, gene expression is mainly controlled by the *cis*-regulatory system (CRS) and transcription factor (TF) proteins that bind specifically to DNA sites [1]. The TFs influence the transcription rate by interacting with other transcriptional components (RNA polymerase, TATA-binding protein, etc.). Like any molecular interaction, the binding of TFs to the regulatory sites is a stochastic event rendering the transition between states of the CRS a stochastic process. This source of noise is known as intrinsic noise in gene expression regulation to distinguish it from that produced by other influences such as random fluctuations in nutrients, cell division or regulatory inputs to the transcriptional machinery, known as extrinsic noise [2,3].

There is a broad variety of different CRS motifs that underlie such regulation. The diversity of CRS ranges from simple ones to more complex motifs that include dozens of regulatory sites, some of them organized in clusters or tandems [1]. This cluster organization points to cooperative effects in the gene regulatory process because proteins rarely seem to bind to DNA without interacting with other DNA-binding proteins. Despite this complexity, the bulk of stochastic models for gene regulation are based on transitions between two promoter states (active and inactive) and, recently, more complex models have been explored [4,5]. All these models approximate the transcriptional control by using a regulatory expression function (Hill function in [6–9] or an *ad hoc* function to fit the model to the experimental data in [4,5]). The approximation assumes that changes in the levels of TF are reflected instantaneously in the transcription rate. Although this approximation could be reasonable to study the static deterministic behavior of transcriptional regulation [8,9], it could lead to a significant underestimation of transcriptional noise [10]. Consequently, these models cannot accurately describe how the overall regulatory process affects noise expression. In this paper, we propose a theoretical model of transcriptional regulation that considers a CRS with several regulatory binding sites for activating proteins. All transition rates between CRS states follow the law of mass action for elementary reactions. In this way, our model accounts for the fact that the expression response is determined by the dynamics of CRS.

II. MODEL

We are interested in exploring how the molecular interaction affects the cooperativity and the fluctuations level of the gene expression. In this sense, we found that stronger interaction between activators increases the level of noise expression. In our model the transcriptional regulation is assumed to be a stochastic process in which the regulatory system makes transitions between different states. The model includes N regulatory binding sites for the same TF (Fig. 1 illustrates the case with three regulatory binding sites). The states $s=1,2,\ldots,N+1$ represent, respectively, states with $0,1,\ldots,N$ binding sites occupied by TFs. The states $s \geq N+2$ correspond to the transcriptional complex formation, where all components required for transcription are as-

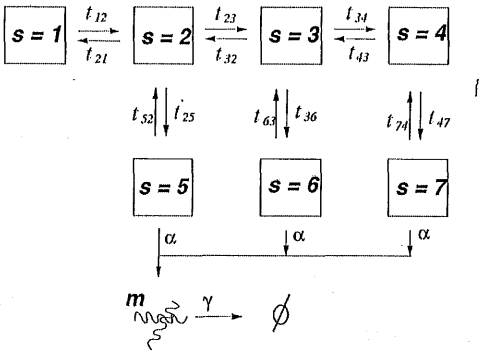

FIG. 1. Kinetic regulatory scheme. All parameters shown in this schematic diagram are constants.

*Author to whom correspondence should be addressed; ldiambra@creg.org.ar

Geometric characteristics of dynamic correlations for combinatorial regulation in gene expression noise

Jiajun Zhang, Zhanjiang Yuan, and Tianshou Zhou
School of Mathematical and Computational Sciences, Sun Yet-Sen University, Guangzhou 510275, People's Republic of China
(Received 16 April 2009; revised manuscript received 28 May 2009; published 7 August 2009)

Knowing which mode of combinatorial regulation (typically, AND or OR logic operation) that a gene employs is important for determining its function in regulatory networks. Here, we introduce a dynamic cross-correlation function between the output of a gene and its upstream regulator concentrations for signatures of combinatorial regulation in gene expression noise. We find that such a correlation function with respect to the correlation time near the peak close to the point of the zero correlation time is always upward convex in the case of AND logic whereas is always downward convex in the case of OR logic, whichever sources of noise (intrinsic or extrinsic or both). In turn, this fact implies a means for inferring regulatory synergies from available experimental data. The extensions and applications are discussed.

DOI: 10.1103/PhysRevE.80.021905 PACS number(s): 87.18.−h, 05.45.Tp, 87.16.Yc

I. INTRODUCTION

Cells live in a complex environment and continuously have to make decisions for different signals that they sense. A challenge in systems biology is to understand how signals are integrated. As the central information-processing units of living cells, transcription regulatory networks allow them to integrate different signals and generate specific responses of genes. The elementary computations are performed at the *cis*-regulatory regions of the genes. The transcription rate of each gene (the output) is a function of the active concentrations of each of the input transcription factors (TFs) [1]. Such a quantitative mapping between the regulator concentrations and the output of the regulated gene is known as the *cis*-regulatory input function (CRIF), which can be modeled by Boolean logics [2,3] in analogy with Boolean calculations that basic electronic devices perform [4]. For example, two activators regulate a gene with AND or OR logic operation (refer to Fig. 1). In fact, AND and OR logic gates are the most frequently accounted instances in the biological literature, surely due to their simplicity and widespread representation in many regulatory processes. For example, the variants of the *lac* promoter display AND and OR behaviors by introducing point mutations [5]. Other examples include that *Pu* variants with stronger binding sequences for specific RNAP make the regulatory module XylR/m-xylene/Pu a robust AND gate [6]; the gene FliLMnoPQR, which makes up the flagella motor, is combinatorially regulated by activator FlhDC and activator FliA with OR logic gate [7]. The notion of logic operations can also be generalized by introducing a continuous function that encodes the dependence of the rate of transcription on the concentrations of inputs [1]. Knowing which mode of combinatorial regulation that a gene employs is important for determining its function in regulatory networks. For example, the *cis*-regulatory module drives cellular patterns differently depending on how the gene integrates intracellular and extracellular signals at its regulatory region by endogenous and exogenous transcription factors [8,9].

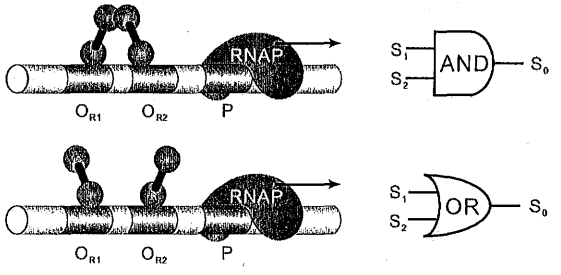

FIG. 1. (Color online) Schematic illustration of *cis*-regulatory constructs. The regulatory functions are realized through the regulated recruitment of transcription factors and RNA polymerase (RNAP).

Experiments performed on single cells have revealed that because TFs are often present in low copy numbers, stochastic fluctuations or noise in the concentrations of these molecules can have significant influences on gene regulation [10–13]. The traditional fluctuation-dissipation relation derived by the linear noise approach [14] based on the master equation gives the information only about the second-order moments. Recently, a modified fluctuation-dissipation relation was derived by Warmflash and Dinner [15], which relates some third-order moments evaluated at the system steady state to the derivatives of a CRIF. Such a *static cross correlation* provides the information only about how three time series are correlated at the zero correlation time. From viewpoints of gene regulation, however, the binding of TFs to the DNA is context dependent, active in some genetic states but not in others. In particular, stochastic fluctuations or "noise" in gene expression propagate from active inputs to the outputs of regulated genes during signal integration. Thus, *dynamic cross correlations* [16,17] would provide a noninvasive means to probe modes of combinatorial regulation in gene expression noise. The purpose of this paper is to demonstrate its potentials in detecting signatures of combinatorial interaction. Regarding the study of combinatorial regulation, there are other works [18–22]. Usually, these papers used some real time-course microarray data to test their algorithms and identify some synergistic TFs, e.g., Chen *et al.* [19], used a kinetic model to select the combinatorial control of multiple TFs: selection of thermodynamic models for combinatorial control of multiple TFs in early differentiation of embryonic stem cell.

Bacterial growth and motility in sub-micron constrictions

Jaan Männik, Rosalie Driessen, Peter Galajda, Juan E. Keymer, and Cees Dekker[1]

Kavli Institute of Nanoscience, Delft University of Technology, Lorentzweg 1, 2628 CJ, Delft, The Netherlands

Communicated by Robert H. Austin, Princeton University, Princeton, NJ, July 10, 2009 (received for review April 18, 2009)

In many naturally occurring habitats, bacteria live in micrometer-size confined spaces. Although bacterial growth and motility in such constrictions is of great interest to fields as varied as soil microbiology, water purification, and biomedical research, quantitative studies of the effects of confinement on bacteria have been limited. Here, we establish how Gram-negative *Escherichia coli* and Gram-positive *Bacillus subtilis* bacteria can grow, move, and penetrate very narrow constrictions with a size comparable to or even smaller than their diameter. We show that peritrichously flagellated *E. coli* and *B. subtilis* are still motile in microfabricated channels where the width of the channel exceeds their diameters only marginally (~30%). For smaller widths, the motility vanishes but bacteria can still pass through these channels by growth and division. We observe *E. coli*, but not *B. subtilis*, to penetrate channels with a width that is smaller than their diameter by a factor of approximately 2. Within these channels, bacteria are considerably squeezed but they still grow and divide. After exiting the channels, *E. coli* bacteria obtain a variety of anomalous cell shapes. Our results reveal that sub-micron size pores and cavities are unexpectedly prolific bacterial habitats where bacteria exhibit morphological adaptations.

biophysics | confinement | microbiology | microfluidics

Bacterial growth and movement in confined spaces is ubiquitous in nature and plays an important role in diverse fields ranging from soil microbiology, water purification, to microbial pathogenesis. The majority of bacteria in soil and bedrock live in pores of size 6 micrometer and smaller (1). These bacteria constitute a large portion of the Earth's biomass (2) and are essential for the functioning of soil. Although distributions of bacteria in soil and Earth's subsurfaces have been studied, it is largely unknown how bacteria grow, move, and penetrate pores of very small size. The latter is also an important question for water treatment and purification. Whereas microbiology textbooks consider output from 0.2-μm pore size filters sterile, it has recently been found that numerous bacteria can pass through these membranes and grow thereafter (3, 4). It is unclear what mechanism bacteria employ to penetrate such membranes. Also, in microbial pathogenesis, bacterial growth and penetration is a problem, for example in dental implants (5), but likely also in soft tissues and bones of a host organism where confined spaces are relevant to bacterial propagation through the extracellular matrix.

Some experimental (6–10) and theoretical (11, 12) studies have discussed the effects of restricting geometry on bacterial motility. It has been established that *Escherichia coli* bacteria can swim in 2.0 μm and wider channels without appreciable slowdown (8) and that bacteria regularly swim in close proximity to surfaces (9), preferring some types of surfaces to others (10). It has been shown that these behaviors can be used to guide bacterial movement in microfluidic structures (10, 13). The effects of confinement on bacterial growth have received very limited attention. Growth of *E. coli* bacteria has been studied by Takeuchi et al. in microfabricated structures (14). In these experiments, confinement affected bacterial growth in the direction of its elongation. The experiments showed that the filamentous bacteria can bend during growth and conform to the shapes of the microfabricated structures. All previous research on bacterial motility and growth have been carried out in relatively large channels and constrictions where the critical dimension is larger than one micrometer, that is, larger than bacterial diameter. So far, no one has addressed questions such as: How narrow channels can bacteria penetrate using their own motility? How do bacterial movement and growth change in very narrow channels compared with that in unbound medium?

Here, we establish how *E. coli* and *Bacillus subtilis* bacteria can grow and move in very narrow constrictions with sub-μm width, and we determine the lower limits for the constriction size which these bacteria are able to penetrate. We show that *E. coli* and *B. subtilis* retain their motility in microfabricated channels with a width that exceeds their diameters by only approximately 30%. We also show that bacteria can penetrate even narrower channels. To achieve this, bacteria initiate growth into the channels. In this process, elongation and division pushes bacteria forward until they fill the whole channel. Whereas *B. subtilis* bacteria can grow in such a way in channels as narrow as their diameter, *E. coli* bacteria are even able to penetrate channels with a width that is much smaller than their diameter. Our work demonstrates that growth in channels which are narrower than the bacterial diameter can drastically change the shape of *E. coli* and lead to a morphological phenotype which has not been described previously.

Results

To carry out this study, we design and fabricate microfluidic channels (constrictions) which connect chambers (small bacterial wells) on a silicon chip and image individual GFP-labeled bacteria in these structures using fluorescent time-lapse microscopy. The advantages of using silicon chips for these experiments are the possibility to define sub-micrometer size channels and the capability to carry out long-term measurements with these bacteria. Whereas the bacteria can pass wide channels within seconds, it can take several days before the bacteria are able to cross the narrowest channels. The microfluidic chips that we use make it possible to maintain the necessary conditions for bacterial growth and motility for such periods of time. The schematic of the microfluidic chip used in this experiment is presented in Fig. 1*A*. The motile bacteria enter the structure of chambers and channels from the left vertical channel. The observations start when the bacteria reach to the left-most chamber of the structure and start to move through the channels toward the chambers on the right end of the arrays. Bacterial movement in channels is partially driven by chemotaxis toward the nutrient source which consists of growth media in the 'feeding channel' on the right end of the arrays. From left to right, the channels are fabricated progressively narrower. This allows monitoring how the population of bacteria is able to negotiate increasingly narrower channels and adapt to life in such a confined environment. On the same silicon chip, a large

Author contributions: J.M., P.G., J.E.K., and C.D. designed research; J.M. performed research; J.M. and R.D. analyzed data; and J.M., P.G., J.E.K., and C.D. wrote the paper.

The authors declare no conflict of interest.

Freely available online through the PNAS open access option.

[1]To whom correspondence should be addressed. E-mail: c.dekker@tudelft.nl.

This article contains supporting information online at www.pnas.org/cgi/content/full/0907542106/DCSupplemental.

Bacterial growth and motility in sub-micron constrictions

Jaan Männik, Rosalie Driessen, Peter Galajda, Juan E. Keymer, and Cees Dekker[1]

Kavli Institute of Nanoscience, Delft University of Technology, Lorentzweg 1, 2628 CJ, Delft, The Netherlands

Communicated by Robert H. Austin, Princeton University, Princeton, NJ, July 10, 2009 (received for review April 18, 2009)

In many naturally occurring habitats, bacteria live in micrometer-size confined spaces. Although bacterial growth and motility in such constrictions is of great interest to fields as varied as soil microbiology, water purification, and biomedical research, quantitative studies of the effects of confinement on bacteria have been limited. Here, we establish how Gram-negative *Escherichia coli* and Gram-positive *Bacillus subtilis* bacteria can grow, move, and penetrate very narrow constrictions with a size comparable to or even smaller than their diameter. We show that peritrichously flagellated *E. coli* and *B. subtilis* are still motile in microfabricated channels where the width of the channel exceeds their diameters only marginally (~30%). For smaller widths, the motility vanishes but bacteria can still pass through these channels by growth and division. We observe *E. coli*, but not *B. subtilis*, to penetrate channels with a width that is smaller than their diameter by a factor of approximately 2. Within these channels, bacteria are considerably squeezed but they still grow and divide. After exiting the channels, *E. coli* bacteria obtain a variety of anomalous cell shapes. Our results reveal that sub-micron size pores and cavities are unexpectedly prolific bacterial habitats where bacteria exhibit morphological adaptations.

biophysics | confinement | microbiology | microfluidics

Bacterial growth and movement in confined spaces is ubiquitous in nature and plays an important role in diverse fields ranging from soil microbiology, water purification, to microbial pathogenesis. The majority of bacteria in soil and bedrock live in pores of size 6 micrometer and smaller (1). These bacteria constitute a large portion of the Earth's biomass (2) and are essential for the functioning of soil. Although distributions of bacteria in soil and Earth's subsurfaces have been studied, it is largely unknown how bacteria grow, move, and penetrate pores of very small size. The latter is also an important question for water treatment and purification. Whereas microbiology textbooks consider output from 0.2-μm pore size filters sterile, it has recently been found that numerous bacteria can pass through these membranes and grow thereafter (3, 4). It is unclear what mechanism bacteria employ to penetrate such membranes. Also, in microbial pathogenesis, bacterial growth and penetration is a problem, for example in dental implants (5), but likely also in soft tissues and bones of a host organism where confined spaces are relevant to bacterial propagation through the extracellular matrix.

Some experimental (6–10) and theoretical (11, 12) studies have discussed the effects of restricting geometry on bacterial motility. It has been established that *Escherichia coli* bacteria can swim in 2.0 μm and wider channels without appreciable slowdown (8) and that bacteria regularly swim in close proximity to surfaces (9), preferring some types of surfaces to others (10). It has been shown that these behaviors can be used to guide bacterial movement in microfluidic structures (10, 13). The effects of confinement on bacterial growth have received very limited attention. Growth of *E. coli* bacteria has been studied by Takeuchi et al. in microfabricated structures (14). In these experiments, confinement affected bacterial growth in the direction of its elongation. The experiments showed that the filamentous bacteria can bend during growth and conform to the shapes of the microfabricated structures. All previous research on bacterial motility and growth have been carried out in relatively large channels and constrictions where the critical dimension is larger than one micrometer, that is, larger than bacterial diameter. So far, no one has addressed questions such as: How narrow channels can bacteria penetrate using their own motility? How do bacterial movement and growth change in very narrow channels compared with that in unbound medium?

Here, we establish how *E. coli* and *Bacillus subtilis* bacteria can grow and move in very narrow constrictions with sub-μm width, and we determine the lower limits for the constriction size which these bacteria are able to penetrate. We show that *E. coli* and *B. subtilis* retain their motility in microfabricated channels with a width that exceeds their diameters by only approximately 30%. We also show that bacteria can penetrate even narrower channels. To achieve this, bacteria initiate growth into the channels. In this process, elongation and division pushes bacteria forward until they fill the whole channel. Whereas *B. subtilis* bacteria can grow in such a way in channels as narrow as their diameter, *E. coli* bacteria are even able to penetrate channels with a width that is much smaller than their diameter. Our work demonstrates that growth in channels which are narrower than the bacterial diameter can drastically change the shape of *E. coli* and lead to a morphological phenotype which has not been described previously.

Results

To carry out this study, we design and fabricate microfluidic channels (constrictions) which connect chambers (small bacterial wells) on a silicon chip and image individual GFP-labeled bacteria in these structures using fluorescent time-lapse microscopy. The advantages of using silicon chips for these experiments are the possibility to define sub-micrometer size channels and the capability to carry out long-term measurements with these bacteria. Whereas the bacteria can pass wide channels within seconds, it can take several days before the bacteria are able to cross the narrowest channels. The microfluidic chips that we use make it possible to maintain the necessary conditions for bacterial growth and motility for such periods of time. The schematic of the microfluidic chip used in this experiment is presented in Fig. 1*A*. The motile bacteria enter the structure of chambers and channels from the left vertical channel. The observations start when the bacteria reach to the left-most chamber of the structure and start to move through the channels toward the chambers on the right end of the arrays. Bacterial movement in channels is partially driven by chemotaxis toward the nutrient source which consists of growth media in the 'feeding channel' on the right end of the arrays. From left to right, the channels are fabricated progressively narrower. This allows monitoring how the population of bacteria is able to negotiate increasingly narrower channels and adapt to life in such a confined environment. On the same silicon chip, a large

Author contributions: J.M., P.G., J.E.K., and C.D. designed research; J.M. performed research; J.M. and R.D. analyzed data; and J.M., P.G., J.E.K., and C.D. wrote the paper.

The authors declare no conflict of interest.

Freely available online through the PNAS open access option.

[1]To whom correspondence should be addressed. E-mail: c.dekker@tudelft.nl.

This article contains supporting information online at www.pnas.org/cgi/content/full/0907542106/DCSupplemental.